The Moss Growth Optimization (MGO): Concepts and performance

Boli Zheng[1], Yi Chen[1], Chaofan Wang[1], Ali Asghar Heidari[2], Lei Liu[3] and Huiling Chen[1,*]

[1] Key Laboratory of Intelligent Informatics for Safety & Emergency of Zhejiang Province, Wenzhou University, Wenzhou 325035, China

[2] School of Surveying and Geospatial Engineering, College of Engineering, University of Tehran, Tehran, Iran

[3] College of Computer Science, Sichuan University, Chengdu, Sichuan 610065, China

∗ Corresponding author. chenhuiling.jlu@gmail.com

Abstract

The moss growth optimization (MGO), introduced in this paper, is an algorithm inspired by the moss growth in the natural environment. The MGO algorithm initially determines the evolutionary direction of the population through a mechanism called the determination of wind direction, which employs a method of partitioning the population. Meanwhile, drawing inspiration from the asexual reproduction, sexual reproduction, and vegetative reproduction of moss, two novel search strategies, namely spore dispersal search and dual propagation search, are proposed for exploration and exploitation, respectively. Finally, the cryptobiosis mechanism alters the traditional metaheuristic algorithm's approach of directly modifying individuals' solutions, preventing the algorithm from getting trapped in local optima. In experiments, a thorough investigation is undertaken on the characteristics, parameters, and time cost of the MGO algorithm to enhance the understanding of MGO. Subsequently, MGO is compared with ten original and advanced CEC 2017 and CEC 2022 algorithms to verify its performance advantages. Lastly, this paper applies MGO to four real-world engineering problems to validate its effectiveness and superiority in practical scenarios. The results demonstrate that MGO is a promising algorithm for tackling real challenges. The source codes of the MGO are available at https://aliasgharheidari.com/MGO.html and other websites.

Keywords: Metaheuristic; Optimization; Swarm intelligence; Moss growth optimization; Engineering design problems

1. Introduction

Proposing new metaphor-based algorithms merely is not a proper direction (Villalón et al., 2020), while designing efficient optimization models can be a step forward in addressing the complexity of new feature spaces. In essence, it is not about novelty but rather the accuracy, performance, and adaptability of tools developed and at which level it can decode the complexities of the new data terrain. Some of these methods may not be an original model, but they employed a new metaphor and a comparable structure and procedures to formerly existing approaches. In addition, the use of metaphor is not an advantage, while if there is any metaphor that helps understand underlying mechanisms, it is not a drawback. This study tries its best to introduce an effective optimization tool, emphasizing its model performance and computational features. The proposed method utilizes a metaphor to describe the process more clearly but is not supposed to be its advantage; we utilized many benchmark functions to provide insight into the potential and drawbacks of its performance and results.

Optimization methods have been a widespread topic in dealing with single objective, multi-objective and many objective classes in recent years (Cao, Zhao, et al., 2020; Cao et al., 2019). In single objective cases, the scenario is simpler than many objective problems, but then the searching logics in single objective methods can be generalized to develop many objective variants (Cao, Wang, et al., 2020). In this regard, many logics have been utilized aiming for finding better solutions in dealing with real-world cases (Y. Duan et al., 2023). For example, large neighborhood search was a successful logic that has been utilized for many real-world cases (Xu & Wei, 2023). Metaheuristic algorithms (MAs) are optimization logics explicitly designed to ascertain approximate solutions for complex global optimization problems (Jia & Lu, 2024). Typically, these algorithms do not depend on the inherent structural characteristics of the given problems; instead, they exhibit remarkable versatility and robustness, enabling them to effectively traverse solution spaces in uncertain environments to identify global optima or near-optimal solutions (Peng et al., 2023). Fundamental characteristic of MAs resides in their ability to integrate global random search with local search strategies, enabling them to simulate the intelligent phenomena found in nature, such as biological evolution, physical processes, and animal swarm behavior.

Through an iterative process, these algorithms persistently explore uncharted areas of the solution space while concurrently attempting to refine and improve upon the currently discovered solutions.

In recent years, there has been an increasing focus on exploring and implementing MAs. This surge in interest can primarily be attributed to the inherent benefits that these algorithms can offer for single objective, multi-objective, and many objective problems (Cao, Wang, et al., 2020; Bin Cao et al., 2021). Firstly, the scalability of MAs is remarkably high, enabling its applicability to both linear and nonlinear problems, as well as single and multi-mode scenarios and problems of varying dimensions (Sahoo et al., 2023). Secondly, the application of MAs is straightforward, as they can be designed and implemented directly, even without knowledge of the derivative of the objective function (Sun et al., 2019). Compared to mathematical methods and traditional optimization algorithms (Qiao et al., 2024; Zhao et al., 2024), MAs can, to some extent, overcome the challenges associated with the vast complexity of mathematical reasoning, potential determinism, and other issues (Li et al., 2023). Thirdly, MAs demonstrate significant computational efficiency, typically requiring fewer computational resources than precise optimization methods, making them suitable for solving large-scale optimization problems (Zhang et al., 2024).

MAs find extensive applications in diverse domains. Specifically, within the realm of medical image segmentation, MAs served the purpose of identifying the most advantageous combination of thresholds for multi-threshold images (Guo et al., 2024; Sahoo et al., 2023). In the domain of engineering optimization, MAs were employed to ascertain the parameters in the implementation engineering to enhance the design (Ferahtia et al., 2023; Matoušová et al., 2023). In the realm of deep learning, MAs were employed to refine the quantity of hyperparameters or neural network nodes within a model (Asif et al., 2023; Emam et al., 2023). In machine learning, MAs were utilized to select crucial data features (Meola et al., 2023; Xie et al., 2023).

Many MAs have been made known, with a wide range of sources for inspiration. However, this source is not the main point to focus on it, as the main key is the mathematical model and performance features of the MAs. This paper categorizes MAs into four distinct classifications, considering the variations in the phenomena they have encountered (Rajwar et al., 2023). These categories include evolutionary algorithms, swarm intelligence algorithms, physical law-based algorithms, and miscellaneous algorithms. Figure 1 visually illustrates the classification of MAs.

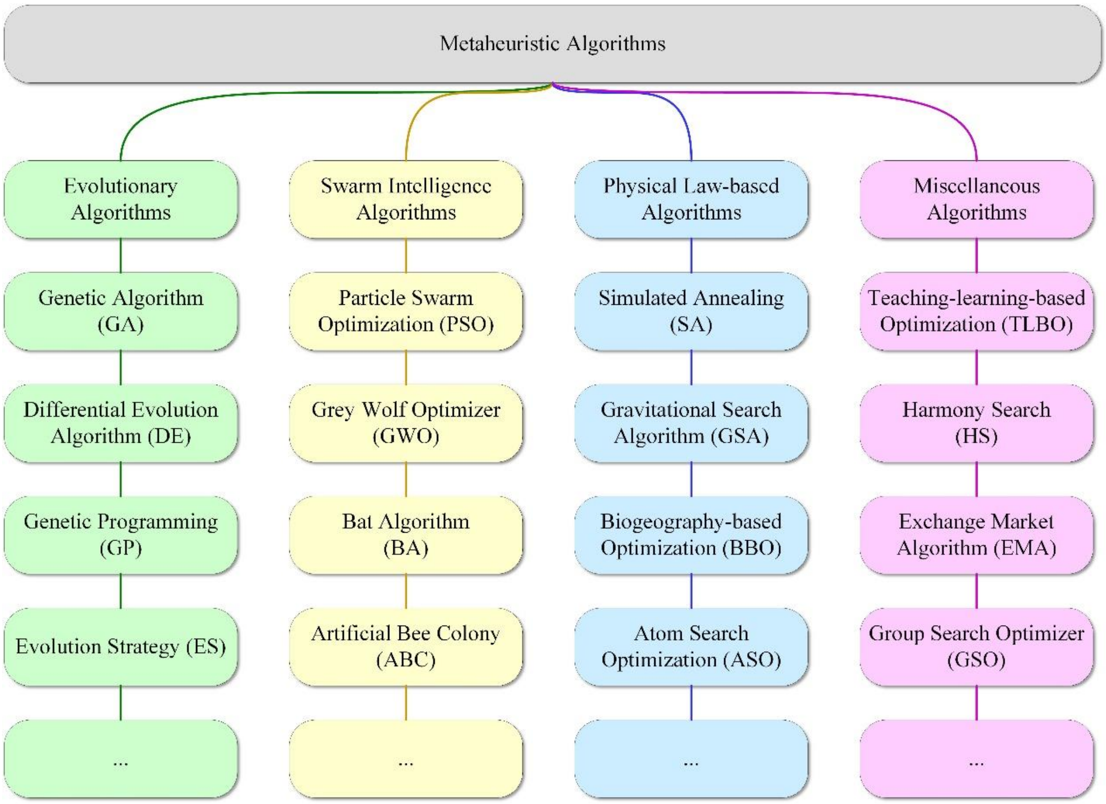

Figure 1. Classification of MAs.

The evolutionary algorithms, which are regarded as the earliest MAs, draw inspiration from the processes of natural selection and the fundamental principles of genetics. These algorithms necessitate the construction of an accumulation of potential solutions and subsequently iteratively apply designated operators to produce novel candidate solutions. The genetic algorithm (GA) (Holland, 1992) stands as the earliest and most renowned algorithm in this domain. Through a sequence of operations such as selection, recombination, and mutation, GA generates new solutions and subsequently assesses and selects solutions using fitness functions. The differential evolution algorithm (DE) (Storn & Price, 1997) is also a type of evolutionary algorithm. DE generally exhibits superior performance compared to GA (Wang et al., 2022). Furthermore, several other evolutionary algorithms have been proposed, such as genetic programming (GP) (Koza, 1994), evolution strategy (ES) (Beyer & Schwefel, 2002), and human evolutionary optimization algorithm (Lian & Hui, 2024).

Swarm intelligence algorithms represent a significant division of MAs, with most MAs falling under this particular category. A swarm intelligence algorithm serves as an optimization and calculation technique, drawing inspiration from the conduct of various natural organisms, including but not limited to ants, bees, fish, and birds. This algorithm category mimics the process by which a collective of organisms can effectively address intricate problems through uncomplicated interactions among a crowd of individuals (Wang & Zhang, 2023). Despite the individual limitations, the collective as a whole demonstrates remarkable intelligence and optimized behavior. Particle swarm optimization (PSO) (B. Cao et al., 2021) represents a traditional group intelligence algorithm. Each "particle" possesses both speed and position, and its state of motion is consistently updated by considering its historical optimal solution and the global optimal solution to discover the global optimal solution within the problem space. Additionally, there exist several other swarm intelligence algorithms, including grey wolf optimizer (GWO) (Mirjalili et al., 2014), bat algorithm (BA) (Yang & Hossein Gandomi, 2012), artificial bee colony (ABC) (Karaboga, 2005), coati optimization algorithm (Dehghani et al., 2023), greylag goose optimization (El-kenawy et al., 2024), spider wasp optimizer (Abdel-Basset et al., 2023). Any of these methods, has its own limitations and weaknesses that make them inefficient in dealing with some complex problems (Yin et al., 2020).

Physical law-based algorithms, which constitute the third type of MAs, draw inspiration from various physical phenomena, including attraction, repulsion, and gravity. Additionally, these algorithms incorporate principles from chemical processes, such as chemical reactions and molecular interactions. An exemplary algorithm that exemplifies this approach is simulated annealing (SA) (Kirkpatrick et al., 1983). SA employs the principles of energy conversion and system balance, observed in solid annealing processes in the physical realm. By doing so, SA has devised a method that effectively avoids local optimization and instead identifies global optimal solutions in intricate search spaces. Other physical law-based algorithms include the gravitational search algorithm (GSA) (Rashedi et al., 2009), biogeography-based optimization (BBO) (Simon, 2008), atom search optimization (ASO) (Zhao et al., 2019), artificial physics algorithm (APA) (Xie et al., 2009), artificial chemical process (ACP) (Irizarry, 2004), ions motion optimization (IMOA) (Javidy et al., 2015), and thermal exchange optimization (TEO) (Kaveh & Dadras, 2017). However, some of these methods cannot perform strong in multimodal problems, while others may converge to local optima, rapidly (Wang et al., 2017).

This article categorizes various heuristic phenomena, including human behavior, game strategies, mathematical theorems, and more, as part of the miscellaneous algorithms. These algorithms form the basis for these heuristic phenomena and are relatively new, presenting innovative perspectives for advancing MAs. The teaching-learning-based optimization (TLBO) (Rao et al., 2011) method replicates the process of student teaching in a classroom setting. This algorithm draws inspiration from the educational concepts of "learning from teachers" and "learning from peers", which involve collaboration and knowledge exchange among individuals with varying levels of expertise and understanding. There are also other algorithms, such as harmony search (HS) (Geem et al., 2001), exchange market algorithm (EMA) (Ghorbani & Babaei, 2014), group search optimizer (GSO) (He et al., 2009), and mother optimization algorithm (Matoušová et al., 2023). Convergence to wrong best solutions, immature performance, weak results, and imbalance of local search and global search are some of observed weaknesses in this group (Luo et al., 2024). Also, some of these methods may not be an original model, but they used a new metaphor and a similar structure and operations to previously existing methods.

Significant research has been conducted on original MAs and their advancements within the past few years (Sun et al., 2018). Whether it is imperative to propose novel algorithms is an issue that necessitates resolution. The field of MAs is still in its early stages compared to physics, chemistry, or mathematics (Rajwar et al., 2023). Hence, despite numerous MAs, due to the lack of solid theoretical backing, enhancing MAs can be achieved through the continuous presentation of innovative concepts to attain superiority. Furthermore, while certain algorithms demonstrate success in benchmarking functions, they are highly ineffective when applied to real-world problems. No free lunch (NFL) theory (Wolpert & Macready, 1997) supports the notion that a special algorithm cannot adapt to all forms of optimization problems and still shows best performance. With the rapid advancement of various fields, numerous challenging optimization problems continue to emerge. Existing optimization techniques may not be sufficient to solve these problems satisfactorily, necessitating the development of new optimization techniques to address them. In specific fields, many scholars have proposed algorithm improvements, such as multi-level threshold image segmentation (Hao et al., 2023; Qian et al., 2023), feature selection (Hussein et al., 2023; Kundu & Mallipeddi, 2022), and combinatorial optimization problem (S. Duan et al., 2023; Wang et al., 2024). Lastly, the innovative ideas of some new algorithms can offer new models and views to enhance existing optimization algorithms. Existing MAs have their strengths and limitations, providing valuable insights and aiding in developing more advantageous MAs. Scholars can design faster and more efficient optimization algorithms by introducing novel ideas and techniques. The emergence of hybrid MAs is the strongest evidence (Bouaouda & Sayouti, 2022; Jaafari et al., 2019; Ngo et al., 2022).

Existing metaheuristic algorithms have certain limitations when dealing with complex optimization problems, such as (a) the presence of overly complex functions, which can cause the algorithm to get stuck in local optima; (b) low computational efficiency; and (c) declining performance in high-dimensional search spaces. This paper presents a useful swarm intelligence algorithm called moss growth optimization (MGO), inspired by the pattern of moss growth in nature. Unlike traditional MAs, MGO divides the population into major individuals according to dimensions and calculates the evolution direction of the population based on the gap between the best individual and the major. This mechanism is significantly different from that of other MAs. Based on this method, MGO is comprised of three primary mechanisms: spore dispersal search, dual propagation search, and cryptobiosis mechanism. Additionally, one of the core ideas of MGO is the determination of wind direction, which significantly impacts the overall evolution of the population. Inspired by the dispersal of moss spores, spore dispersal search includes two types of steps that correspond to the different performances of spores in stable winds and turbulent winds, which are beneficial for conducting global searches in different ranges. Dual propagation search combines sexual reproduction and vegetative reproduction in moss, achieving local exploitation of the algorithm through computations with the optimal individual. The cryptobiosis mechanism changes the traditional approach of directly modifying the individual solutions and replaces the greedy selection mechanism, preventing the algorithm from getting trapped in local optimal solutions.

In the experiments, qualitative analysis was initially conducted to analyze the characteristics of MGO. Afterward, to validate the performance of MGO, comparisons were made between MGO and 10 original algorithms as well as 10 advanced algorithms in the CEC 2017 (Wu et al., 2017) and CEC 2022 (Ahrari et al., 2022). Furthermore, parameter sensitivity analysis was conducted to determine the optimal parameters MGO used and analyze the suitable problem scale employed by MGO. Lastly, the running time of MGO was analyzed, and MGO was applied to 4 engineering optimization problems.

In summary, the contributions of this paper are as follows:

1. Based on natural phenomena, a useful metaheuristic algorithm called moss growth optimization has been proposed, drawing inspiration from the growth patterns of moss.

2. A mechanism called the determination of wind direction is suggested. It provides a useful approach for MAs by dividing and calculating the mean of the optimal individuals to determine the evolution direction of the population.
3. The spore dispersal search technique is employed for global exploration, whereas the development strategy utilizes dual propagation search for local exploitation. The mechanism of cryptobiosis alters the method of directly updating individual solutions.
4. Through conducting qualitative analysis experiments and parameter sensitivity experiments, the algorithmic attributes of MGO are thoroughly described to enhance its applicability to a wide range of optimization problems.
5. A comparison experiment was carried out to assess the effectiveness of MGO compared to 20 other algorithms using a set of benchmark functions, thus demonstrating the advantages of MGO.
6. The MGO algorithm has been utilized in four real-world engineering optimization problems, initially presenting the algorithm's capability to address practical optimization problems.

The remaining sections of this paper are structured as follows. Section 2 presents the natural occurrence of moss growth in relation to MGO and the comprehensive mathematical model of the MGO algorithm. Section 3 presents a sequence of experiments combined with analysis, including qualitative analysis, performance comparison experiments, parameter sensitivity analysis, time spent analysis, and experiments on engineering design problems. Section 4 concludes the entire paper and provides insight into future improvements and applications of MGO.

2. Moss growth optimization

This section will initially introduce the source of inspiration derived from moss and subsequently introduce the mathematical models of the algorithm.

2.1 Inspired from moss

Moss is one of the oldest types of land plants on Earth (Heckman et al., 2001). It commonly thrives in damp and shaded locales; nevertheless, it demonstrates resilience in diverse settings, ranging from wooded areas to metropolitan regions (Schaefer & Zrÿd, 2001). Although lacking flowers, fruits, seeds, roots, or true vasculature (Lueth & Reski, 2023), this plant relies on distinctive mechanisms for reproduction. Specifically, they have three modes of reproduction: asexual, sexual, and vegetative. Additionally, cryptobiosis serves as a critical survival strategy that contributes to the perpetuation of the species.

(a) gametophytes of moss (b) sporophytes of moss

Figure 2. Different stages of moss.

Moss exhibits a peculiar phenomenon known as heteromorphic alternation of generations, whereby the sporophyte and gametophyte stages alternate (Cove, 2005; Reski, 1998), as shown in Figure 2[1]. Sporophytes of moss release spores, which subsequently develop into new moss individuals called the gametophytes. This process coincides with asexual reproduction in moss. Moss spores are mainly released in the morning when wind speeds are relatively low (Johansson et al., 2016). Furthermore, spores released under stable wind conditions in the morning tend to travel more distances than those dispersed later in the day under more turbulent winds. This suggests that morning winds provide more favorable conditions for spore dispersal. Figure 3 demonstrates the dispersal of spores in stable and turbulent winds. Figure 3a illustrates that the spores exhibit a consistent trajectory and disperse over long distances in stable winds. Conversely, Figure 3b demonstrates that spores display erratic trajectories and disperse only over short distances in turbulent winds.

[1] Pictures obtained from https://pixabay.com/ as copy right free images
(a) https://pixabay.com/photos/moss-star-moss-forest-plant-2683009/
(b) https://pixabay.com/photos/moss-nature-brick-wall-illuminated-7342179/.

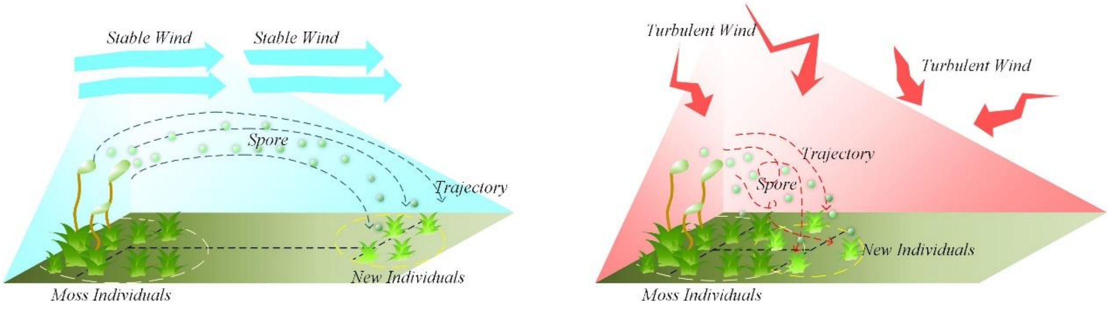

(a) spore dispersal in stable wind

(b) spore dispersal in turbulent wind

Figure 3. Dispersal of spores in stable and turbulent winds.

Sexual reproduction of moss requires free-motile sperm to travel from male to female gametophytes (Rosenstiel et al., 2012). When the sperm, aided by water droplets present on the moss, attach to the eggs and fertilize them, they form zygotes. These zygotes further develop into the sporophytes of moss. The sporophyte depends on the gametophyte for nourishment and remains attached to it. Simultaneously, gametophytes that inhabit more favorable surroundings are inclined to yield sporophytes (Johnson & Shaw, 2016). The phenomenon of sporophyte growth is visually depicted in Figure 4. It is assumed that as one moves closer to the center of the depicted figure, the environmental conditions become more suitable for moss. Hence, the moss at the center is more inclined to foster sporophytes. In addition, gametophytes can contribute genes to sporophytes when produced through sexual reproduction.

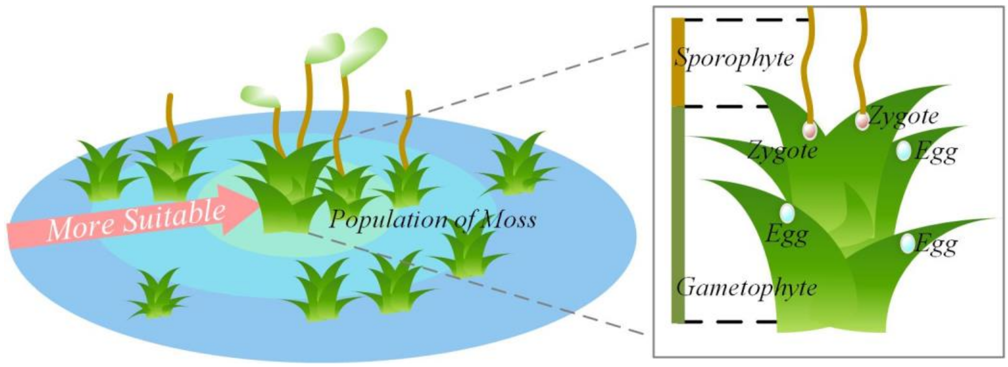

Figure 4. Growth of sporophytes.

The regeneration of vegetative material is common in many moss species, with some shedding fragments that can form the basis of new individuals (Lueth & Reski, 2023). Figure 5 illustrates that shedding fragments of moss are dispersed to various locations through the influence of wind, where they subsequently develop into new individuals. Notably, the dispersal of fragments tends to be more localized than the dispersal of spores.

Cryptobiosis refers to a state of life that is reversible ametabolic, distinguished by the cessation of all metabolic processes (Cannone et al., 2017). This peculiar state enables mosses to endure periods of highly challenging conditions. Furthermore, mosses possess the capacity to revive when conditions become suitable again.

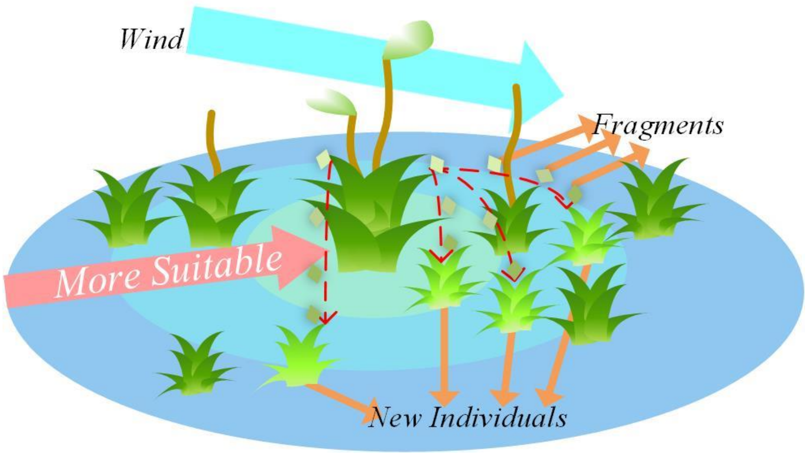

Figure 5. Vegetative reproduction.

In summary, this paper is inspired by the growth mechanism of moss and proposes a useful algorithm named the MGO method. This algorithm incorporates a spore dispersal search for global search space exploration. Subsequently, a dual propagation search is introduced to facilitate local exploitation, which simulates both sexual reproduction and vegetative reproduction. Lastly, a cryptobiosis mechanism is presented as an improved greedy selection mechanism.

2.2 Mathematical model and optimization algorithm

In this section, based on the growth model formulated by moss, this paper first presents the four key stages: determination of wind direction, spore dispersal search, dual propagation search, and cryptobiosis mechanism. Among them, determining wind direction is the most critical mechanism, and it decides the evolutionary direction of the population. Subsequently, we introduce the MGO algorithm.

2.2.1 Determination of wind direction

The growth of moss is influenced by the presence of wind, primarily due to the crucial role wind plays in the dispersal of spores. Due to the significance of wind direction, MGO has developed a creative mechanism called "determination of wind direction." This mechanism utilizes the position relationship between most individuals and the optimal individual to determine the evolutionary direction of all individuals in the population. This evolutionary direction effectively helps MGO avoid trapping into local optimum solutions. It should be noted that the MGO algorithm considers a single moss individual as a search agent M. The algorithm's population X is comprised of all moss individuals. In this paper, to emulate the wind direction by relying on the following assumptions made by the MGO algorithm:

1. The wind direction remains constant throughout an entire iteration.
2. Assuming that moss individuals represent the positions within the solution space, the current best candidate position corresponds to the current moss individual in the optimal solution.
3. The direction of the wind always blows from areas with a higher quantity of moss towards the individual moss in the most favorable growth environment.

The most exceptional individual within the population X is M_{best}. This paper employs the *j*-dimensional value of M_{best} as a threshold and compare the *j*-dimensional values of all individuals with it. Based on this comparison, $DX_{j1} = \{M_i = (M_{i,1}, M_{i,2}, \ldots, M_{i,dim}) | M_{i,j} \geq M_{best,j}, M_i \in X\}$ and $DX_{j2} = \{M_i = (M_{i,1}, M_{i,2}, \ldots, M_{i,dim}) | M_{i,j} < M_{best,j}, M_i \in X\}$ are partitioned, where $M_{i,j}$ is the *j*-th particle of the *i*-th moss individual, and dim is the dimension of moss individual. Then, the set with the larger number of members is selected, as illustrated in Eq. (1).

$$divX_j = \begin{cases} DX_{j1}, & count(DX_{j1}) \geq count(DX_{j2}) \\ DX_{j2}, & count(DX_{j1}) < count(DX_{j2}) \end{cases} \tag{1}$$

where function $count(\cdot)$ indicates calculating the quantity of moss individuals in a given collection of sets.

For sets acquired subsequent to numerous divisions, refer to Eq. (2).

$$divX = \{M_i = (M_{i,1}, M_{i,2}, \ldots, M_{i,dim}) \mid M_i \in \bigcap_{j=1}^{dn} divX_{p_j}, M_i \in X\} \tag{2}$$

where dn denotes the number of times to be divided, and in this paper the value of dn is set to $\lfloor dim/4 \rfloor$ and is not less than 1. $\lfloor \cdot \rfloor$ denotes the floor function of the enclosed number. p_j represents the *j*-th random number, conforming to a range $(1,2, \ldots, dim)$, and satisfies Eq. (3).

$$\bigcap_{j=1}^{dn} p_j = \emptyset \tag{3}$$

In this paper, a brief simulation of the wind is performed, where the wind always comes from the region $divX$ to the most exceptional individual M_{best}, as illustrated in Figure 6. The precise computation of the wind's direction is demonstrated in Eq. (4).

$$D\_wind = \frac{1}{num} \sum_{i=1}^{mum} dM_i, dM_i \in dirX \tag{4}$$

where D_wind represents the calculated wind direction, which has the same dimension as the individuals. The variable num indicates the total number of individuals in the $dirX$. The calculation of $dirX$ can be observed in Eq. (5). The reason for calculating the mean distance between major individuals and M_{best} is that this method can help smooth the path of individuals approaching M_{best}, thereby enhancing the optimization ability of MGO.

$$dirX = \{M_{best} - M_i | M_i \in divX\} \tag{5}$$

where $dirX$ denotes the collection of distances that separate individuals within the $divX$ with respect to M_{best}.

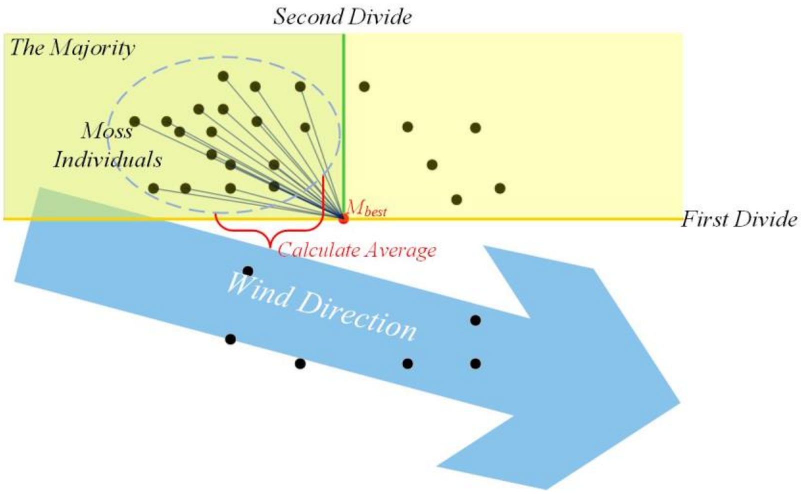

Figure 6. The process of wind direction.

2.2.2 Spore dispersal search

The exploration phase of the MGO involves the spore dispersal search. In situations where there is a significant presence of wind, the dispersal of spores occurs in a highly unpredictable manner, resulting in a substantial transmission distance. Under stable wind conditions, spores are capable of traveling a greater distance, whereas under turbulent conditions, they tend to disperse over shorter distances. The majority of spores are dispersed in stable wind conditions, while a minor portion disperses during turbulent conditions. Ultimately, as wind strength diminishes, spores begin to settle in closer proximity to the moss.

In this paper, the position of spores is considered a new solution. Modeling is conducted to simulate the dispersal characteristics of spores through wind, as shown in Figure 7. The position of spores is determined in Eq. (6). The difference in the size of the two steps is significant. This allows individuals to make random choices to prevent fixed step lengths from causing slow convergence in the early stages of failure to converge in the later stages, ensuring population diversity.

$$M_i^{new} = \begin{cases} M_i + step1 \cdot D\_wind, & r_1 > d_1 \\ M_i + step2 \cdot D\_wind, & r_1 \leq d_1 \end{cases} \tag{6}$$

where M_i^{new} denotes a novel moss that is acquired through the dispersal of spores from *i*-th moss individual M_i. r_1 is a random number in the range $(0,1)$, while d_1 is a constant parameter that is set to 0.2 in this paper. If $r_1 > d_1$, Spores disperse under stable wind conditions, whereas they disperse under turbulent conditions. $step1$ represents the distance of spore dispersal in stable wind conditions, as shown in Eq. (7). $step2$ represents the distance of spore dispersal in turbulent wind conditions, as shown in Eq. (8).

$$step1 = w \cdot (r_2 - 0.5) \cdot E \tag{7}$$

where w is a constant parameter that is set to 2 in this paper. r_2 is a random vector in the range $(0,1)$, which has the same dimension as D_wind. E is the strength of wind, which diminishes as the iterations progress, as shown in Eq. (9).

$$step2 = 0.1 \cdot w \cdot (r_3 - 0.5) \cdot E \cdot [1 + \frac{E}{2} \cdot (1 + \tanh \beta \sqrt{1 - \beta^2})] \tag{8}$$

where r_3 is a random vector in the range $(0,1)$, which has the same dimension as D_wind. The values for β is shown in Eq. (10).

$$E = 1 - \frac{FEs}{MaxFEs} \tag{9}$$

where FEs denotes the present count of evaluations, while $MaxFEs$ signifies the maximum number of iterations.

$$\beta = \frac{count(divX)}{count(X)} \tag{10}$$

where β represents the proportion of the population in $divX$ to the population in X.

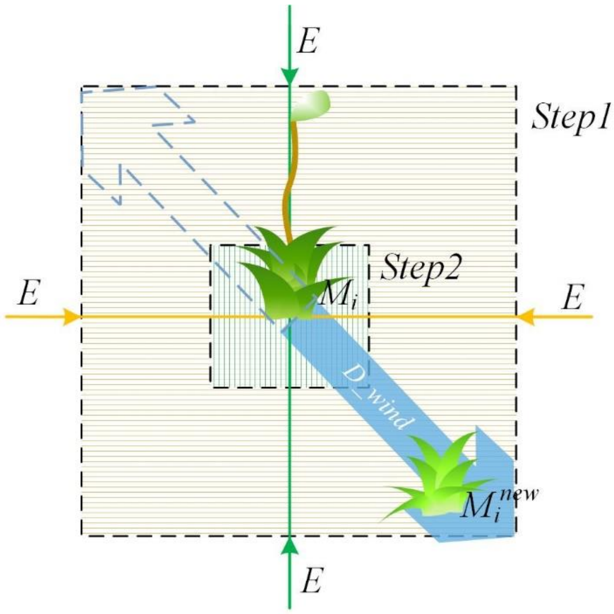

Figure 7. Search process of spore dispersal search.

2.2.3 Dual propagation search

The exploitation phase of the MGO involves the dual propagation search, which simulates both sexual reproduction and vegetative reproduction, resulting in new individuals, created through sexual and vegetative reproduction, who are located close to the original individual. It should be noted that when utilizing dual propagation search, the condition $c < 0.8$ must be satisfied, where c represents a random number within the range $(0,1)$. During sexual reproduction, individual genes are used as solutions, allowing new individuals to acquire genes from current and the best individuals. During vegetative reproduction, fragments from moss individuals can develop into new individuals, which is considered a new solution. The dispersal of fragments, similar to the dispersal of spores, is also influenced by the wind. Compared to spore dispersal, the method of dual propagation search allows moss to reproduce within a more confined area, yet it facilitates the rapid identification of the optimal habitat for the moss.

An imitation is performed on the dual propagation search, as shown in Figure 8. And the position of new moss individual is determined in Eq. (11). The method differs from traditional MAs in that it increases the proportion of methods that only change one individual dimension, strengthening the overall local exploration ability.

$$\begin{cases} M_i^{new} = (1 - act) \cdot M_i + act \cdot M_{best}, & r_4 > d_2 \\ M_{i,j}^{new} = M_{best,j} + step3 \cdot D\_wind_j, & r_4 \le d_2 \end{cases} \tag{11}$$

where M_i^{new} denotes the i-th new individual, $M_{i,j}^{new}$ denotes the j-th particle in M_i^{new}, and j is a random number that does not surpass the maximum dimension of the individual. The current optimal individual is represented by M_{best}. $M_{best,j}$ represents the j-th particle in M_{best}. D_wind_j is the j-th particle in D_wind. r_4 is a random number in the range (0,1). d_2 is a constant parameter that is set to 0.5 in this paper. If $r_4 > d_2$, dual propagation search is simulated in the sexual reproduction stage, whereas it is simulated with a different calculation in the vegetative reproduction stage. Then act evaluates whether the particles within the M_{best} are being utilized, and it is shown in Eq. (12). Finally, the calculation of $step3$ is shown in Eq. (13).

$$act = \begin{cases} 1, & \dfrac{1}{1.5 - 10 \cdot r_5} \geq 0.5 \\ 0, & \dfrac{1}{1.5 - 10 \cdot r_5} < 0.5 \end{cases} \tag{12}$$

where r_5 is a random vector in the range (0,1), which has the same dimension as M_{best}.

$$step3 = 0.1 \cdot (r_6 - 0.5) \cdot E \tag{13}$$

where r_6 is a random number in the range (0,1), and E is the strength of wind.

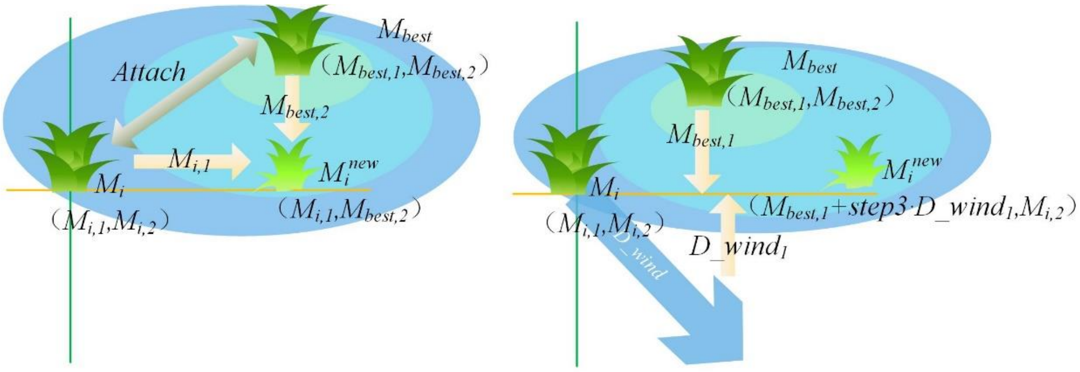

(a) sexual reproduction stage (b) vegetative reproduction stage

Figure 8. Search process of dual propagation search.

2.2.4 Cryptobiosis mechanism

This paper proposes a useful mechanism named the cryptobiosis mechanism to improve the greedy section mechanism. The phenomenon of cryptobiosis refers to the capability of moss to restore and flourish following a period of inactivity or aridity. Where moss confronts arid circumstances or loses its water supply, it desiccates and enters a state of metabolic dormancy. Once conditions become favorable, moss has the ability to revive.

Inspired by the phenomenon of cryptobiosis, this paper proposes a mechanism for recording the historical information of moss individuals. This method differs from the conventional method, in which individuals are directly altered. Instead, this mechanism keeps a record of the moss individuals produced in each iteration. Once certain conditions are met, such as reaching the maximum number of records (which is set to 10 in this paper) or concluding the population iteration, the mechanism is triggered to revive the optimal individual and replace the current one. On one hand, the cryptobiosis mechanism enables moss individuals to explore repeatedly from the same location, thus ensuring the ability of the entire population to explore globally. On the other hand, moss individuals can be replaced under certain conditions, thereby guaranteeing the population's quality.

The general process of cryptobiosis mechanism can be seen in Figure 9. For the i-th individual M_i within the moss population, M_i corresponds to the *0*-th record. The remaining nine records are labeled as rM_i^e, where e denote the e-th record of M_i. It is evident that the 7th record rM_i^7 obtains the optimal solution. This paper marks the best record as rM_i^{best}, then M_i is modified to rM_i^{best}. The pseudo-code of the cryptobiosis mechanism is shown in Algorithm 1.

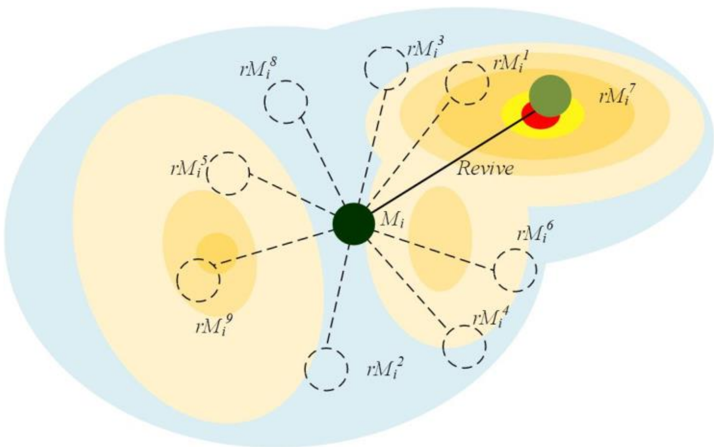

Figure 9. Process of cryptobiosis mechanism.

Algorithm 1: Pseudo-code of cryptobiosis mechanism

---

1. **Input:** M_i: i-th solution
   rec_num: maximum number of records
2. **Output:** Updated M_i
3. $record = 0$
4. **While** $(FEs < MaxFEs)$
5. **If** $record = 0$
6. $rM_i^{record} = M_i$

```
            record = record + 1
        End if
        Update the M_i
        rM_i^record = M_i
        record = record + 1
        If record > rec_num − 1 || t ≥ T
            rM_i^record = M_i
            For e = 1: record
                If Fitness(rM_i^record) < Fitness(rM_i^best)
                    rM_i^best = rM_i^record
                End if
            End for
            M_i = rM_i^best
            record = 0
        End if
        FEs = FEs + N
    End while
    Return M_i
```

2.2.5 Proposed MGO algorithm

In summary, firstly, taking inspiration from the phenomenon governing the dispersal of moss spores through the wind, a mechanism employing two-stage search steps is put forward. This mechanism, named spore dispersal search, is subsequently utilized to conduct global exploration, serving as a fundamental optimization technique within the MGO. Then, drawing inspiration from the sexual and vegetative reproduction of moss, dual propagation search is introduced as another optimization method for the MGO. This mechanism enables effective searching around the optimal individual, which is advantageous for conducting local exploitation searches. Lastly, based on the phenomenon of cryptobiosis of moss, an improved greedy selection mechanism, named cryptobiosis mechanism, is proposed. This mechanism enables multiple explorations of the original individual, thus preventing the trap of local optima and simultaneously enhancing the population's quality.

The MGO algorithm begins by generating a set of random individuals. During each iteration, the population's evolution direction is determined based on determination of wind direction, followed by spore dispersal search. Dual propagation search is performed if $rand < 0.8$, otherwise it is skipped. Individual solutions are updated according to the cryptobiosis mechanism. The overall structure of the algorithm in terms of flow chart and pseudo-code is shown in Figure 10 and Algorithm 2.

2.2.6 The time complexity of MGO

The complexity of MGO mainly includes initialization, fitness calculation, determination of wind direction, spore dispersal search, dual propagation search, and cryptobiosis mechanism. Among them, N denotes the number of moss individuals, D denotes the dimension of the individual, T denotes the maximum number of iterations, and R denotes the maximum number of records of cryptobiosis mechanism. The time complexity of initialization is $O(N)$. The time complexity of fitness calculation is $O(D)$. The time complexity of determining wind direction is $O(N \times D/4)$. The time complexity of the spore dispersal search is $O(N \times D)$. The time complexity of dual propagation search in the two cases is $O(N \times D)$ and $O(N)$. The time complexity of the cryptobiosis mechanism is $O(N \times R)$. Therefore, the overall time complexity of MGO is $O(T \times N \times (D + R + 1))$.

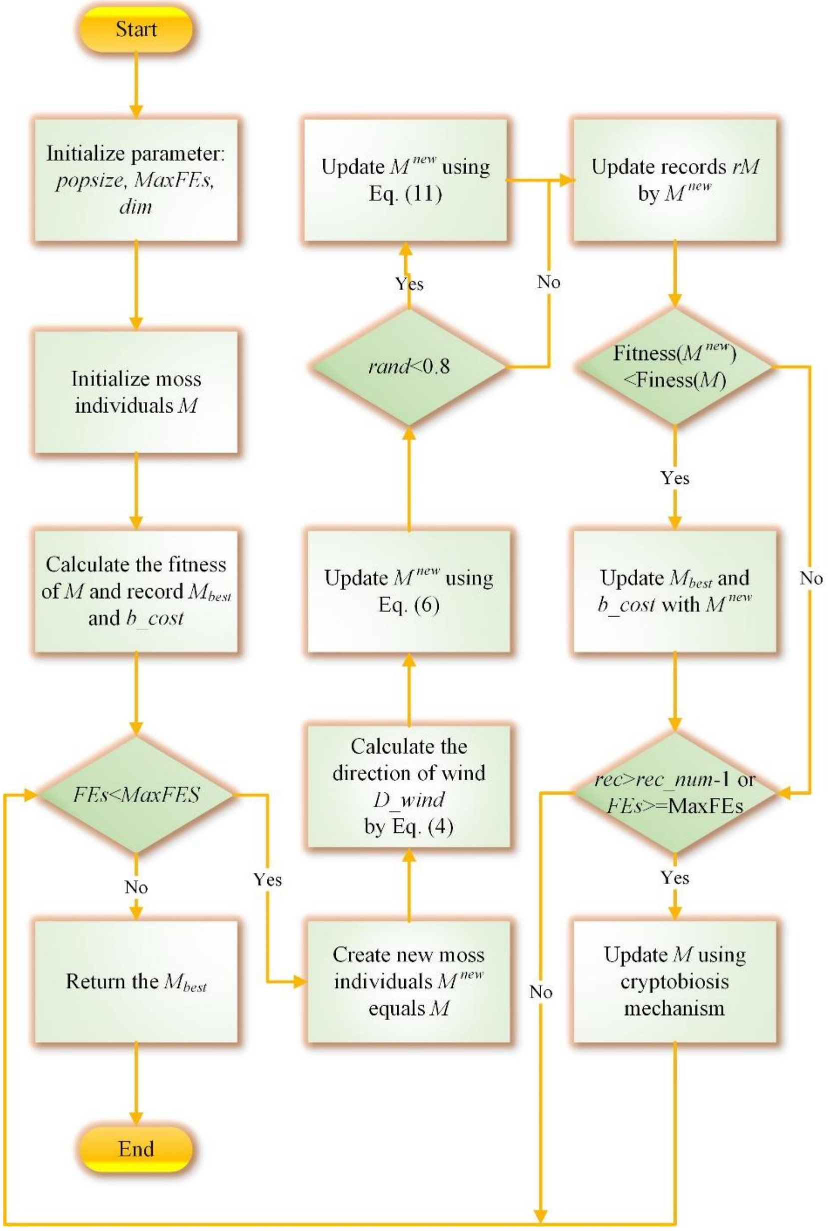

Figure 10. Flowchart of MGO.

Algorithm 2: Pseudo-code of MGO algorithm

---

1. **Input:** N: population size
   dim: the problem dimensions
2. **Output:** Optimal solution
3. **Initialize** a set of M
4. **Calculate** the fitness of M
5. **Calculate** the current optimal agent M_{best} and optimal fitness b_cost
6. **While** $(FEs < MaxFEs)$
7. **Calculate** the wind direction D_wind by Eq. (4)

8. **For** $i = 1:N$
9. **Create** the new search agent M_i^{best} equals M_i
10. **Update** the M_i^{best} by Eq. (6)
11. **If** $rand < 0.8$
12. **Update** M_i^{new} by Eq. (11)
13. **End if**
14. **If** $Fitness(M_i^{new}) < Fitness(M_{best})$
15. $M_{best} = M_i^{new}$
16. $b\_cost = Fitness(M_i^{new})$
17. **End if**
18. **End for**
19. **For** $i = 1:N$
20. **Update** M_i using the cryptobiosis mechanism
21. **End for**
22. $FEs = FEs + N$
23. **End while**
24. **Return** the best solution M_{best}

---

3. Experimental results and analyses

This section carries out a series of experiments to ascertain the advantages and features of the MGO algorithm. Initially, the process of finding the optimal solution of the MGO algorithm is conducted through a quantitative analysis experiment. Subsequently, the MGO algorithm is compared with other peer algorithms to illustrate its performance advantages. The optimal parameters of MGO are then examined through a parameter sensitivity analysis experiment. Furthermore, time spent analysis is employed to analyze the running time of MGO. Ultimately, the application of the MGO algorithm to the engineering optimization algorithm is carried out as a means to showcase the potential of MGO in resolving real-world problems.

In order to guarantee the fairness of the experiments, all experiments were conducted within an identical setting. The experimentation settings include an operating system of Windows 10 22H2 with 16GB RAM, a CPU of 12th Gen Intel (R) Core (TM) i7-12700 (2.10 GHz), and MATLAB R2018b.

3.1 Qualitative analysis of MGO

The qualitative analysis results of MGO for several standard unimodal and multimodal test functions are demonstrated in Figure 11. The functions used for experimental testing are derived from the classical 23 benchmark functions (Yao et al., 1999). This experiment includes four essential indicators: search history, the trajectory of the moss individual in the first dimension, the average fitness of the population, and the convergence curve. For this experiment, the population size of MGO was set to 20, and the algorithm was run for 500 iterations.

In the first instance, by documenting the placement of the optimal individual in every iteration and depicting its position on the corresponding two-dimensional layout, one can visually represent the search history. Utilizing this search history, the characteristics of MGO individuals during the quest for the optimal resolution can be clearly perceived. Subsequently, the trajectory of the moss individual in the first dimension is depicted by recording the first particle of the best individual in each iteration, showcasing the positional changes throughout the iterations. Furthermore, the average fitness value of the population is recorded after each iteration, which in turn facilitates the visualization of the average fitness trend and offers an overview of the population's progression throughout the iterations. Lastly, the fitness of the best individual in each iteration is documented to analyze the overall trend across the iterations within the algorithm.

A depiction of the test function in three-dimensional form is observable in Figure 11a. Then, Figure 11b displays the distribution of historical searches in MGO. It is evident that, apart from a substantial number of clusters in close proximity to the global optimal solution, the optimal solutions also exhibit clusters in various other regions. Moreover, historical optimal solutions are dispersed across a broad spectrum of images, signifying the excellent global search capabilities of MGO, thereby facilitating the discovery of global optimal solutions.

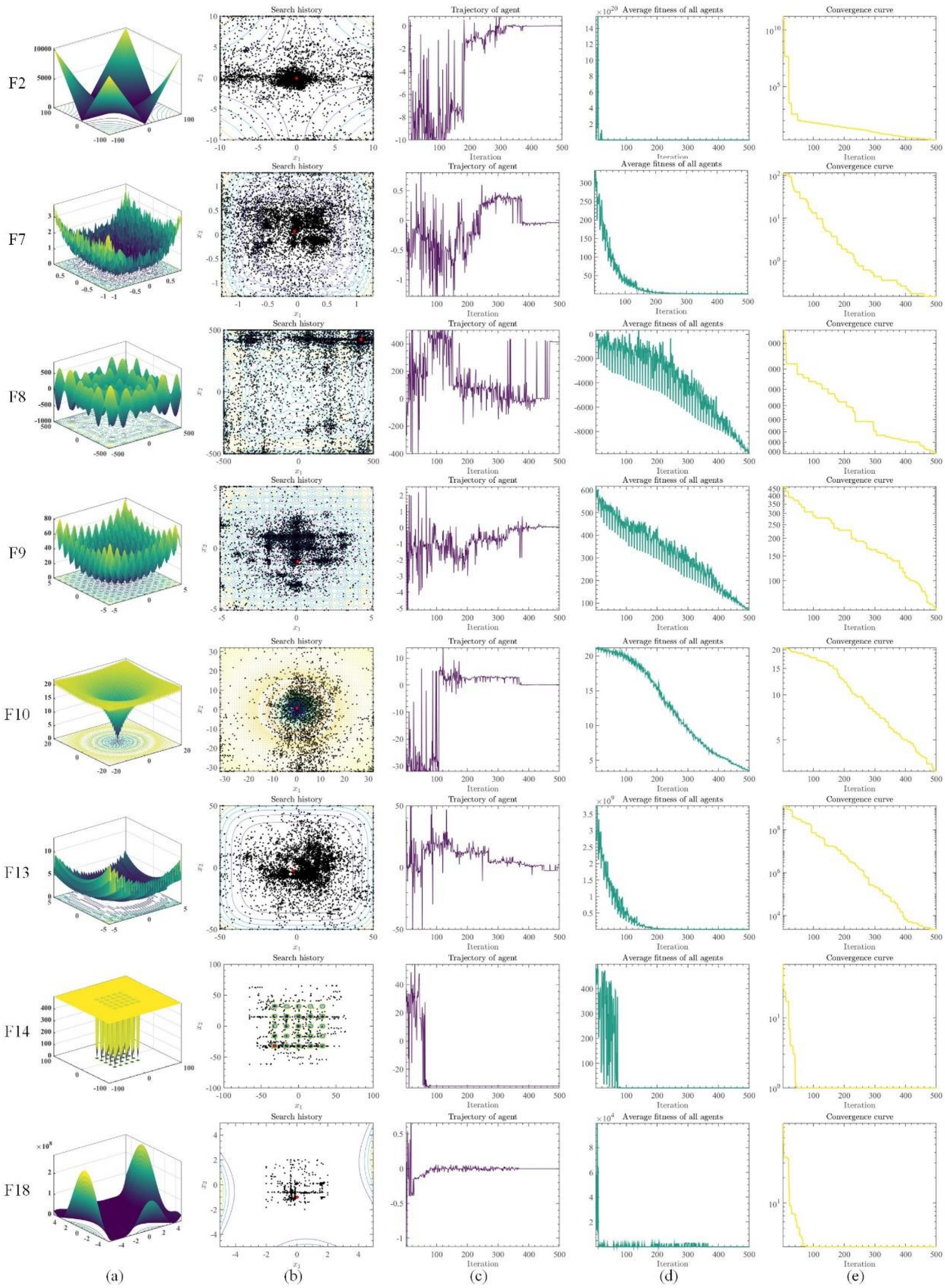

Figure 11. Qualitative analysis experiment of MGO.

Figure 11c illustrates the trajectory of the individual moss in the first dimension. As the iterations progress, the strength of the wind, denoted as E, gradually decreases, leading to a reduction in the search steps. The figure shows that the moss individual took large search steps during the early iterations, particularly in F7, F8, F9, F10, and F13, which approximately encompassed the entire exploration space. This facilitates escaping from local optima. Furthermore, it can be observed that F2, F10, F13, F14, and F18 exhibit a rapid reduction in search steps, indicating that the MGO algorithm possesses favorable adaptability and robustness.

Figure 11d presents the average fitness of the population. It can be observed that, except for F8 and F9, the average fitness of other functions fluctuates less, and the average fitness of all functions shows a decreasing trend, indicating that the quality of the population gradually improves as the iterations proceed.

Figure 11e shows the convergence curve of MGO. Due to the larger strength of the wind E in the spore dispersal search in the early stage, the convergence of the first half of the curve in F9, F10, and F13 is slower. As E it decreases, the convergence speed gradually increases, which is conducive to sufficient search in the early stage and prevents falling into a locally optimal solution. In addition, all functions have a downward trend as a whole, indicating that the combination of spore dispersal search and dual propagation search can effectively find the globally optimal solution.

In conclusion, MGO demonstrates remarkable characteristics, including strong global search capabilities, the ability to escape local optima, good adaptability and robustness, and an effective convergence strategy. These features combine to make MGO a powerful algorithm for finding globally optimal solutions across a range of functions and optimization problems.

3.2 Performance comparison experiment of MGO

In this section, an analysis was conducted to establish the advantage of the GMO algorithm by means of a comparative study against ten original algorithms and ten advanced algorithms.

3.2.1 Comparison with original algorithms on CEC 2017

In this section, a comparison was made between MGO and ten original algorithms that include slime mould algorithm (SMA) (Li et al., 2020), rime optimization algorithm (RIME) (Su et al., 2023), Harris hawks optimization (HHO) (Heidari, Mirjalili, et al., 2019), whale optimization algorithm (WOA) (Mirjalili & Lewis, 2016), PSO (Kennedy & Eberhart, 1995), sine cosine algorithm (SCA) (Mirjalili, 2016), moth-flame optimization (MFO) (Mirjalili, 2015), firefly algorithm (FA) (Yang, 2009), GWO (Mirjalili et al., 2014), and bat algorithm (BA) (Yang, 2010). The default values for the key parameters of the algorithms employed in the comparison were all selected, and comprehensive information regarding these parameters can be found in Table 1. The test functions for comparative analysis originate from CEC

2017 (Wu et al., 2017). The functions from the CEC 2017 are displayed in Table 2, and they encompass a diverse range including unimodal, multimodal, hybrid, and composition functions. It should be noted that the F2 test function in CEC 2017 will not be utilized in this paper due to its inherent instability. Furthermore, the subsequent function numbers will follow the original order of CEC 2017 rather than the order after removing F2. All algorithms were executed in identical conditions to ensure fairness in comparative experiments. The size of population was established at 30, while the dimensions and evaluations count were set at 30 and 300,000 respectively. In order to mitigate the influence of stochastic factors on the outcomes of the algorithms, all the algorithms being compared were independently executed 30 times for each function and the results were averaged to yield the final running outcome.

Table A1 (Appendix) demonstrates the average (Avg) and standard deviation (Std) values of MGO and the original algorithms utilized in the experiment after 30 independent runs. The algorithm's closeness to the optimal solution of the benchmark function can be discerned by observing the smaller Avg value, while a smaller Std value indicates a more consistent and reliable algorithm. Firstly, by observing Avg, it can be seen that aside from the F2 function, MGO has the capability to acquire the minimum Avg value or comes close to the algorithm that acquires the minimum Avg value in most functions. This demonstrates that the MGO algorithm possesses the ability to discover relatively superior solutions in most functions. Moreover, it is evident that MGO is better suited for solving intricate functions than unimodal ones. Subsequently, by observing Std, it can be observed that MGO attains the minimum Std values in 20 functions, indicating that MGO exhibits good stability.

Furthermore, the Wilcoxon signed-rank test (WSRT) (Alcalá-Fdez et al., 2009) is employed to analyze the findings related to MGO and the performance of the original algorithms, as presented in Table 3. The *p*-value is a critical statistical measure in this test as it represents the probability of observing the sample difference or an even more extreme condition, assuming the null hypothesis is true. The calculation of the *p*-value helps us evaluate whether the observed performance difference is likely due to random variation only. If the *p*-value produced by the comparison is less than the significance level of 0.05, it is considered that the discrepancies between the two algorithms are statistically significant. The symbol '+' indicates the number of cases where MGO's overall performance exceeds that of the alternative functions across all test functions. Conversely, the symbol '-' denotes the number of instances where MGO's overall performance is inferior to that of other functions across all test functions. Lastly, the symbol '=' represents the number of cases where MGO's overall performance is comparable to that of the alternative functions. The term 'Avg' indicates the average ranking after 30 iterations of parallelization, while 'Rank' denotes the overall final ranking. It can be discerned that MGO achieves a significantly better ranking than the second-placed algorithm when considering the comprehensive evaluation. Specifically, the mean ranking score of MGO amounts to 1.5517, which is notably superior to that of the runner-up. In detail, MGO outperforms the second-ranked algorithm in the majority of trial functions, specifically in 17 out of the total. Although there are 4 trial functions where MGO performs marginally worse and 8 where its performance is equivalent, these do not significantly impact the overall superior ranking of MGO. Therefore, Friedman's test (FT) (Sheskin, 2003) was employed. The result of FT, as shown in Figure 12, reveals that MGO has achieved a minimum value of 1.97. The results of WSRT and FT demonstrate the consistent excellence of MGO compared to the other algorithms under consideration.

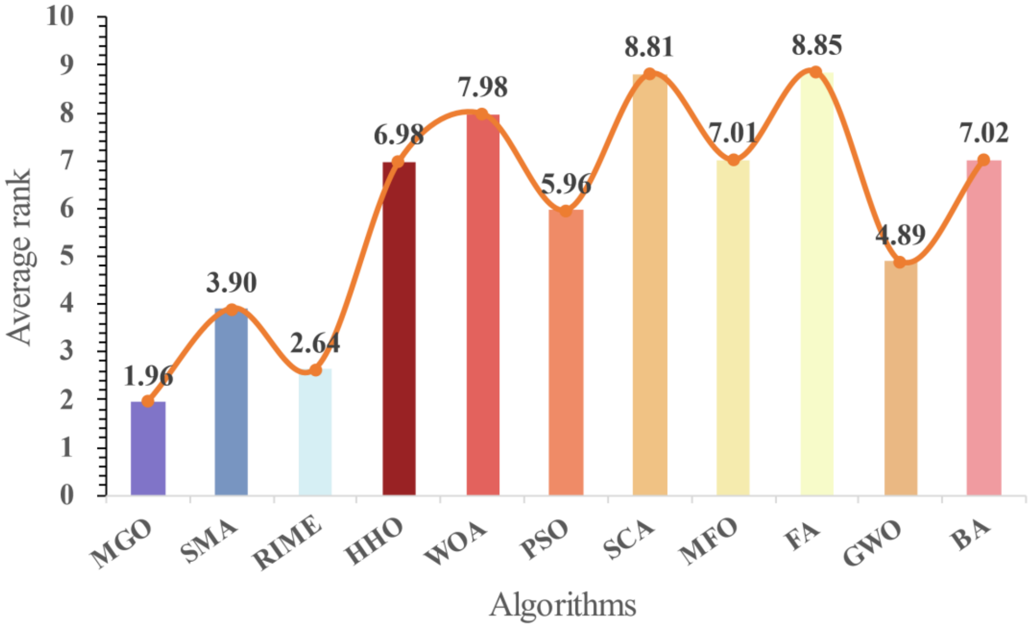

Figure 12. The average ranking of MGO and original algorithms.

In order to gain an intuitive comprehension of the algorithms' convergence, Figure 13 presents the convergence curves of MGO and the original algorithms. In F23 and F24, it is evident that MGO exhibits a stronger ability to converge in the early stages than most algorithms. Based on the final results, MGO achieved the minimum value in all the selected functions, establishing a significant gap with other algorithms in F9, F12, and F22. This provides evidence to support the assertion that the MGO algorithm possesses an advantage in locating a global optimal solution.

In summary, following an experimental comparison with the original algorithms, it has been shown that MGO demonstrates a broad spectrum of applicability. Moreover, the MGO algorithm is better suited for addressing intricate functions than unimodal ones. It exhibits commendable stability, boasts significant advantages over other original algorithms, and ultimately proves to be a highly effective optimization algorithm.

Table 1. Parameters of original algorithms.

Algorithms	Key parameters
SMA	$z = 0.03$
RIME	$W = 5$
HHO	$k = 0$
WOA	$a_1 = [2{,}0];\ a_2 = [-2, -1];\ b = 1$
PSO	$c_1 = 2;\ c_2 = 2;\ vMax = 6$
SCA	$A = 2$
MFO	$b = 1;\ t = [-1{,}1];\ a \in [-1, -2]$
FA	$\alpha = 0.5;\ \beta = 0.2;\ \gamma = 1$
GWO	$a = [2{,}0]$
BA	$A = 0.5;\ r = 0.5$

Table 2. Details of the CEC 2017.

ID	Function Equation	Class	Optimum
F1	Shifted and Rotated Bent Cigar Function		100
F2	Shifted and Rotated Sum of Different Power Function	Unimodal	200
F3	Shifted and Rotated Zakharov Function		300
F4	Shifted and Rotated Rosenbrock's Function		400
F5	Shifted and Rotated Rastrigin's Function	Multimodal	500
F6	Shifted and Rotated Expanded Scaffer's F6 Function		600

6			
F 7	Shifted and Rotated Lunacek Bi-Rastrigin Function		700
F 8	Shifted and Rotated Non-Continuous Rastrigin's Function		800
F 9	Shifted and Rotated Lévy Function		900
F 10	Shifted and Rotated Schwefel's Function		1000
F 11	Hybrid Function 1 (N = 3)	Hybrid	1100
F 12	Hybrid Function 2 (N = 3)		1200
F 13	Hybrid Function 3 (N = 3)		1300
F 14	Hybrid Function 4 (N = 4)		1400
F 15	Hybrid Function 5 (N = 4)		1500
F 16	Hybrid Function 6 (N = 4)		1600
F 17	Hybrid Function 6 (N = 5)		1700
F 18	Hybrid Function 6 (N = 5)		1800
F 19	Hybrid Function 6 (N = 5)		1900
F 20	Hybrid Function 6 (N = 6		2000
F 21	Composition Function 1 (N = 3)	Composition	2100
F	Composition Function 2 (N = 3)		2200

22		
F23	Composition Function 3 (N = 4)	2300
F24	Composition Function 4 (N = 4)	2400
F25	Composition Function 5 (N = 5)	2500
F26	Composition Function 6 (N = 5)	2600
F27	Composition Function 7 (N = 6)	2700
F28	Composition Function 8 (N = 6)	2800
F29	Composition Function 9 (N = 3)	2900
F30	Composition Function 10 (N = 3)	3000

Table 3. Analysis result by using WSRT.

Algorithms	Rank	+/=/-	Avg
MGO	1	~	1.5517
SMA	3	26/2/1	4.0344
RIME	2	17/8/4	2.2068
HHO	6	29/0/0	6.8275
WOA	9	29/0/0	8.4482
PSO	5	23/4/2	5.7586
SCA	11	29/0/0	8.7241
MFO	8	29/0/0	7.4482
FA	10	29/0/0	8.7241
GWO	4	29/0/0	5.0344
BA	7	24/2/3	7.1724

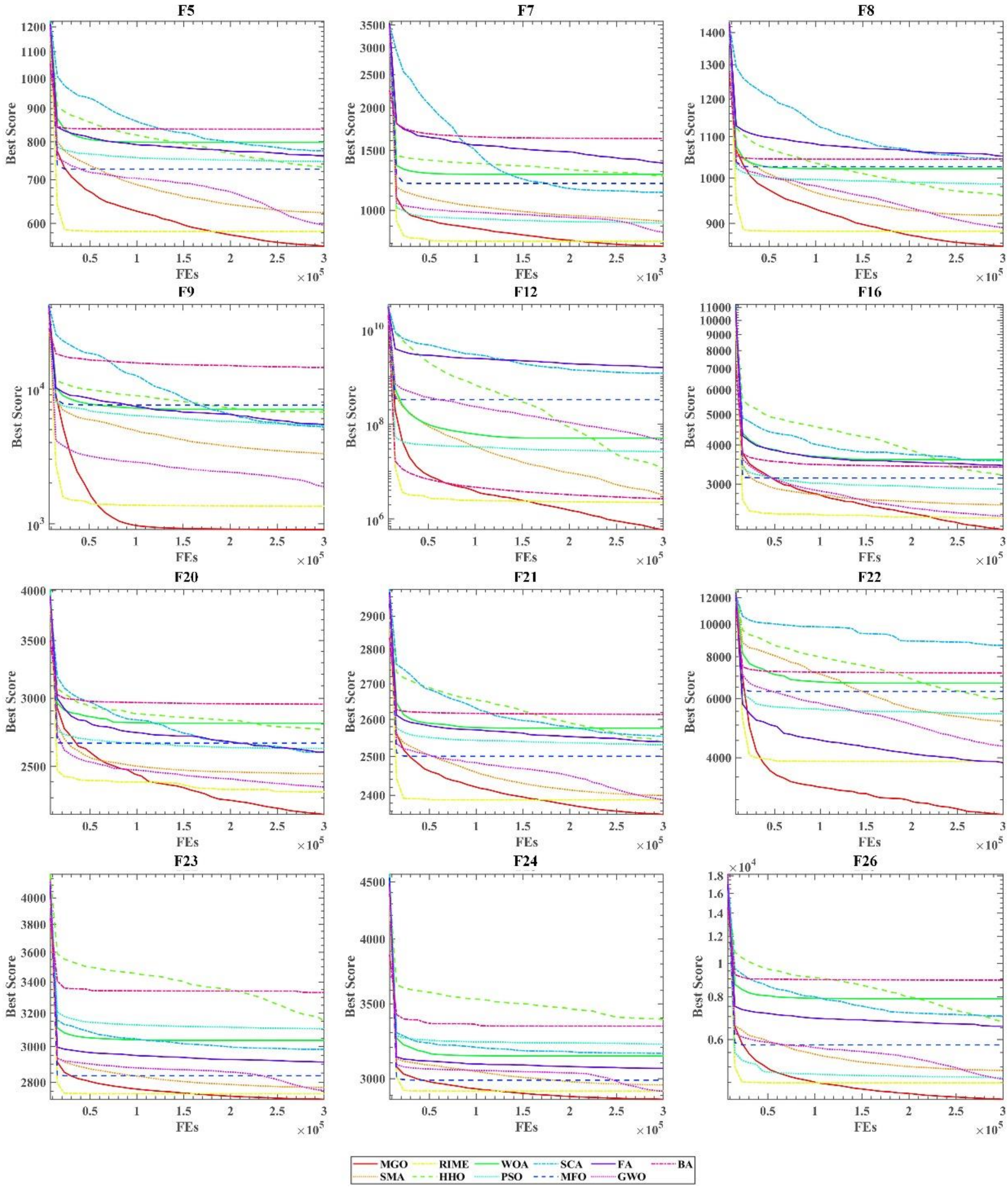

Figure 13. Convergence curves of MGO and original algorithms.

3.2.2 Comparison with advanced algorithms on CEC 2017

In order to further validate the superiority of MGO, in this section, we compared MGO with 10 advanced algorithms, including a hybrid sine-cosine algorithm with a differential evolution algorithm (SCADE) (Nenavath & Jatoth, 2018), improved whale optimization algorithm (IWOA) (Tubishat et al., 2019), hybrid bat algorithm (RCBA) (Liang et al., 2018), opposition-based sine cosine algorithm (OBSCA) (Abd Elaziz et al., 2017), PSO with an aging leader and challengers (ALCPSO) (Chen et al., 2012), completely derandomized self-adaptation in evolution strategies (CMAES) (Hansen & Ostermeier, 2001), boosted GWO

(OBLGWO) (Heidari, Abbaspour, et al., 2019), Cauchy and Gaussian sine cosine optimization (CGSCO) (Kumar et al., 2017), double adaptive random spare reinforced whale optimization algorithm (RDWOA) (Chen et al., 2020), and multi-swarm particle swarm optimization (MSPSO) (Xia et al., 2018). The default parameters as outlined in Table 4 are employed for all algorithms. The test set employed in this study is the CEC 2017. All algorithms in this study have a population size of 30 and a dimension of 30. The number of evaluations conducted is set to 300,000, and these evaluations are performed independently 30 times. Table A2 (Appendix) presents the outcomes of the evaluation using the CEC 2017 dataset, where Avg and Std were examined. The most favorable data points have been highlighted in bold. It can be seen that among the total of 29 functions, MGO achieved both the minimum Avg value and the minimum Std value in the majority of functions, specifically achieving the minimum Avg value in 15 functions and the minimum Std value in 16 functions. Concretely, MGO possesses a significant advantage in multimodal functions, as it is able to achieve the minimum Avg in all multimodal functions except for F6. It still maintains its advantages in hybrid functions and composition functions, achieving five respective minimum Avg values.

Furthermore, the WSRT and FT analysis results can be observed in Table 5 and Figure 14. It is evident that MGO exhibited superior performance compared to advanced algorithms in at least 16 functions. Additionally, MGO attained the lowest average Avg of 1.7 in WSRT, and it obtained the best result of 1.96 in FT. This substantiates that MGO continues to possess commendable advantages compared to advanced algorithms.

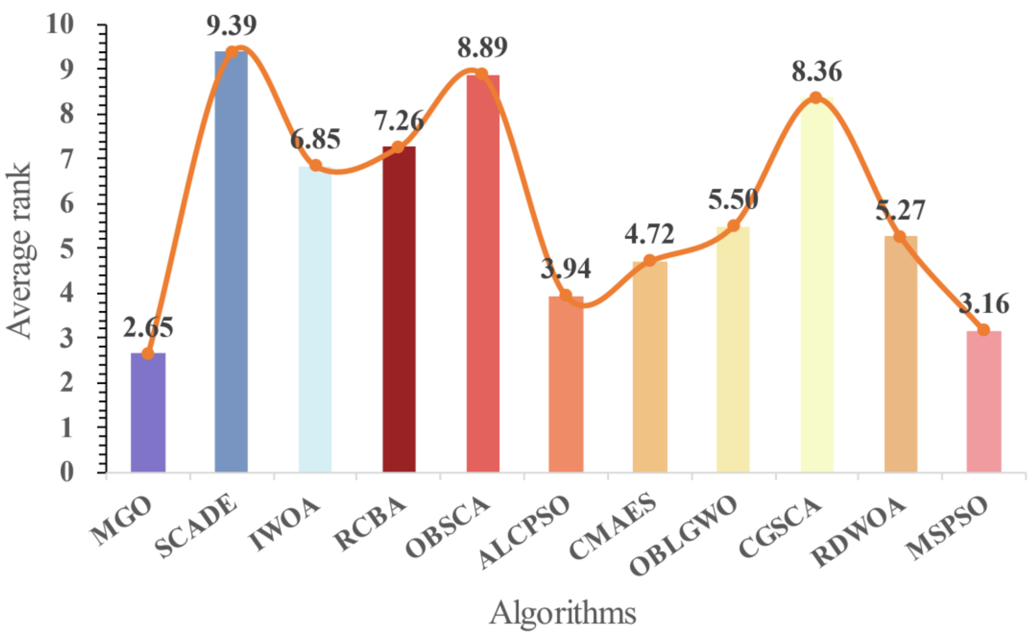

Figure 14. The average ranking of MGO and advanced algorithms.

Figure 15 shows the curve convergence of MGO with other advanced algorithms on CEC 2017. The functions selected for this study demonstrate MGO's remarkable search capability. MGO significantly outperformed other algorithms in F5, F8, F9, F20, and F21. For the remaining functions, MGO consistently performed well. Despite MGO's slightly slower convergence rate in the initial phase, it possesses an effective global search capability.

In conclusion, when compared to advanced algorithms, MGO still maintains its advantages. It has shown a significant advantage in handling multimodal functions. Despite a slightly slower convergence rate during the initial stage, MGO retains its efficient global search capability. MGO is a resilient algorithm that effectively addresses a broad spectrum of optimization problems.

Table 4. Parameters of advanced algorithms.

Algorithms	Key parameters
SCADE	$a = 2;\ F = random\ in\ [0.2,0.8];\ P_c = 0.8$
IWOA	$CR = 0.1;\ b = 1$
RCBA	$Qmin = 0;\ Qmax = 2;\ r = 0.5$
OBSCA	$a = 2$
ALCPSO	$w = 0.4;\ c1 = c2 = 2;\ Age = 0;\ T = 2;\ lifespan = 60$
CMAES	$\sigma = 0.25$
OBLGWO	$\alpha \in [2,0]$
CGSCO	$A = 2$
RDWOA	$A = 2$
MSPSO	$c_1 = 2;\ c_2 = 2;\ vMax = 6.$

Table 5. Analysis result by using WSRT.

Algorithms	Rank	+/=/-	Avg
MGO	1	~	2.2069
SCADE	11	29/0/0	9.7931
IWOA	7	28/1/0	7.1724
RCBA	8	21/5/3	7.4138
OBSCA	10	29/0/0	9.1724
ALCPSO	3	22/4/3	3.5862

CMAES	4	14/2/13	5.0690
OBLGWO	6	28/1/0	5.3793
CGSCO	9	29/0/0	8.1034
RDWOA	5	25/2/2	5.1034
MSPSO	2	16/2/11	3.0000

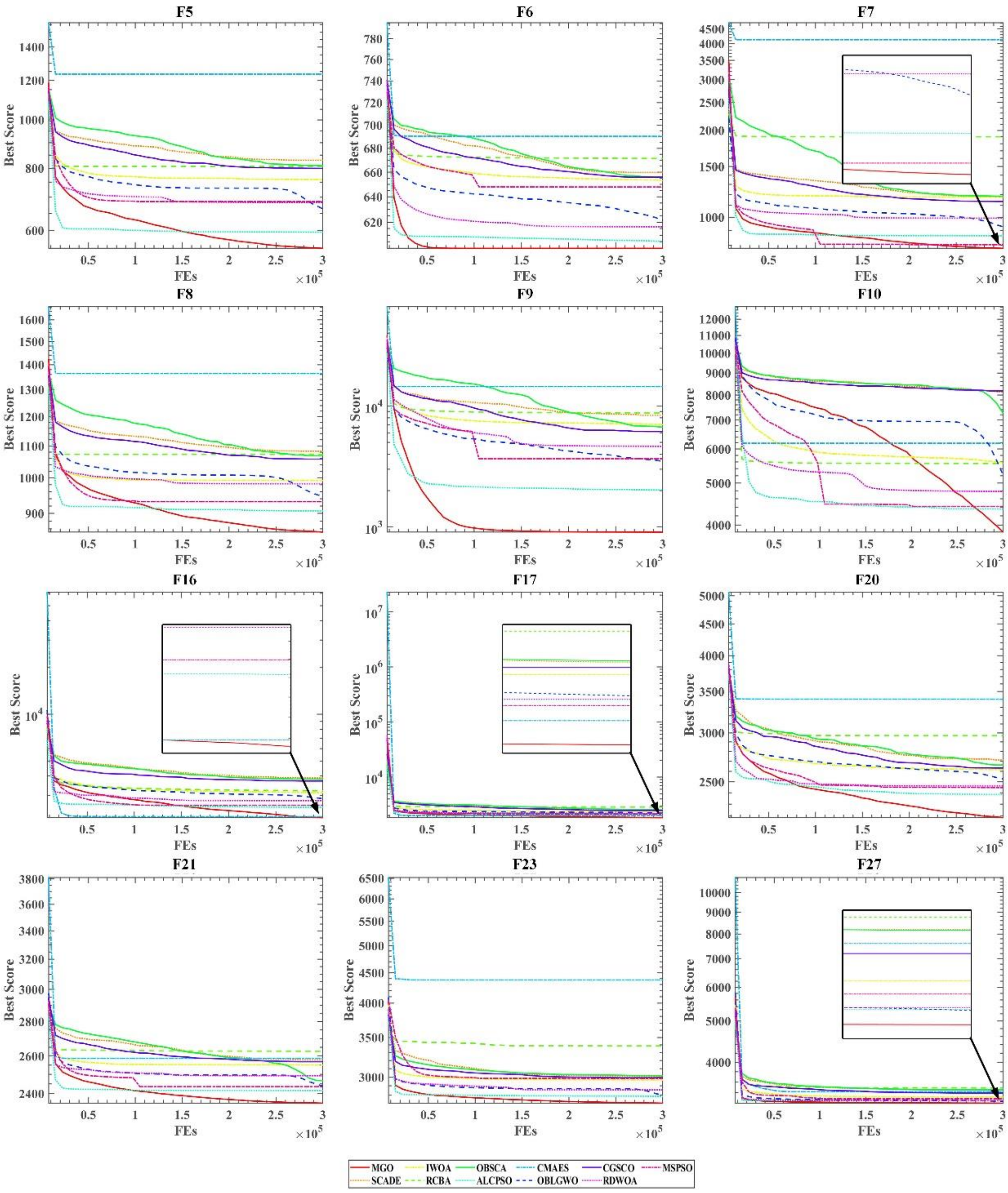

Figure 15. Convergence curves of MGO and advanced algorithms.

3.2.3 Comparison with advanced algorithms on CEC 2017

In order to further illustrate the advantages of MGO and explicate its suitability for a wide range of functions not limited solely to CEC 2017, this section utilizes CEC 2022 (Ahrari et al., 2022) as the experimental test set. The benchmarks within CEC 2022 are detailed in Table 6. The experiment entailed a comparison amongst 10 algorithms. These 10 algorithms were chosen from the above experiments, consisting of 5 original algorithms: RIME, GWO, PSO, WOA, and SCA, as well as 5 advanced algorithms: MSPSO, ALCPSO, IWOA, SCADE, OBLGWO. The selection of these 10 algorithms was based on their strong performance and their representativeness within CEC 2017. The key parameters of each algorithm are set according to the configurations used in the previous experiments. The population size in the experiment is set to 30, and the dimension is set to 20, which is the default value in CEC 2022. The experiment is independently run 30 times with 300,000 evaluations per run.

The Avg and Std of the experimental results obtained from 30 independent trials are provided in Table A3 (Appendix). It is evident from the data that MGO obtained the lowest Avg among the 8 functions and the lowest Std in 6 functions. Regarding the F1 function, while MGO did not achieve the minimum Avg, it is close to the optimal solution for this function. Experiment has validated that MGO exhibits commendable search capability and stability during the CEC 2022. The experimental results, subjected to WSRT analysis, are presented in Table 7. It is apparent that MGO's Avg is 1.75, placing it at the top among all the algorithms compared, and it possesses significant advantages over the other algorithms. Furthermore, when comparing MGO's performance to that of the second-ranked algorithm, RIME, it is evident that MGO outperforms RIME in eight functions. In three functions, the performance of MGO is similar to RIME, while in only one function MGO exhibits inferior performance compared to RIME. The results of the FT analysis can be observed in Figure 16 It can be seen that MGO achieves a minimum value of 2.46, which is proven through FT statistics to establish MGO as the best algorithm among the algorithms being compared. Finally, Figure 17 presents the convergence curves for 6 functions in the experiment. Although MGO's initial convergence rate was slower than that of ALCPSO and RIME, the final results of MGO were superior. Furthermore, MGO has exhibited significant advantages in F4 and F7. This suggests that MGO strikes a favorable balance between exploration and exploitation.

Overall, through many experiments and analyses, it has been demonstrated that MGO not only exhibits advantages at CEC 2017, but also possesses a substantial competitive edge at CEC 2022. This indicates the broad range of applications for MGO.

Table 6. Details of the CEC 2022.

ID	Function Equation	Class	Optimum
F1	Shifted and full Rotated Zakharov Function	Unimodal	300
F2	Shifted and full Rotated Rosenbrock's Function	Multimodal	400
F3	Shifted and full Rotated Expanded Schaffer's f6 Function		600
F4	Shifted and full Rotated Non-Continuous Rastrigin's Function		800
F5	Shifted and full Rotated Levy Function		900
F6	Hybrid Function 1 (N = 3)	Hybrid	1800
F7	Hybrid Function 2 (N = 6)		2000
F8	Hybrid Function 3 (N = 5)		2200
F9	Composition Function 1 (N = 5)	Composition	2300
F10	Composition Function 2 (N = 4)		2400
F11	Composition Function 3 (N = 5)		2600
F12	Composition Function 4 (N = 6)		2700

Table 7. Analysis result by using WSRT.

Algorithms	Rank	+/=/-	Avg
MGO	1	~	1.75
MSPSO	4	7/1/4	5.0833
ALCPSO	3	9/3/0	4.75
IWOA	8	10/2/0	6.75

SCADE	11	12/0/0	9.5
OBLGWO	5	11/1/0	5.5833
RIME	2	8/3/1	2.75
GWO	7	12/0/0	6.6667
PSO	6	9/2/1	6.5833
WOA	10	10/2/0	8.4167
SCA	9	12/0/0	8.1667

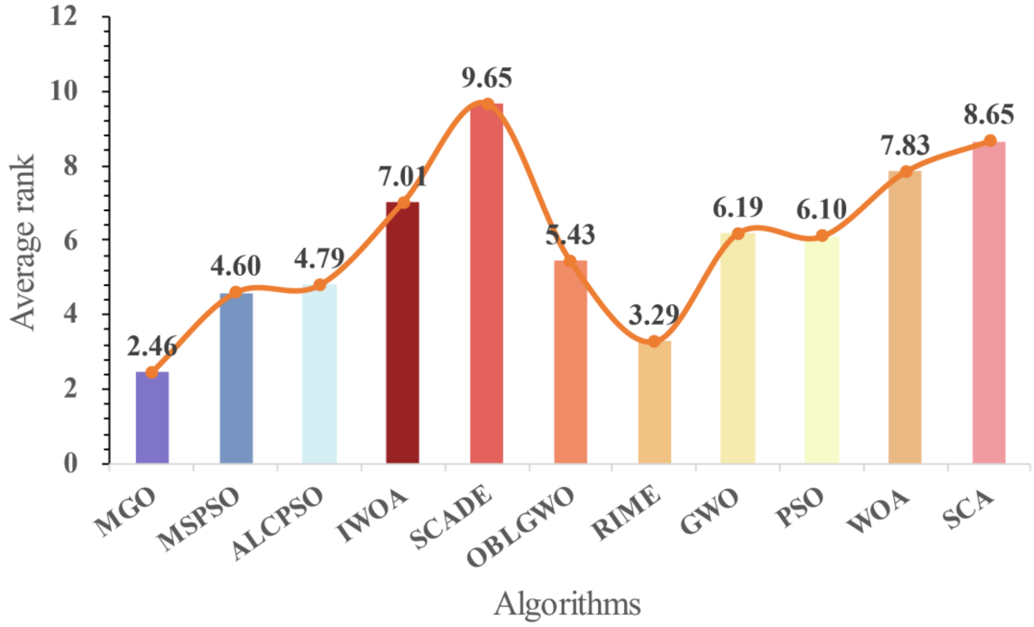

Figure 16. The average ranking of MGO and other algorithms in CEC 2022.

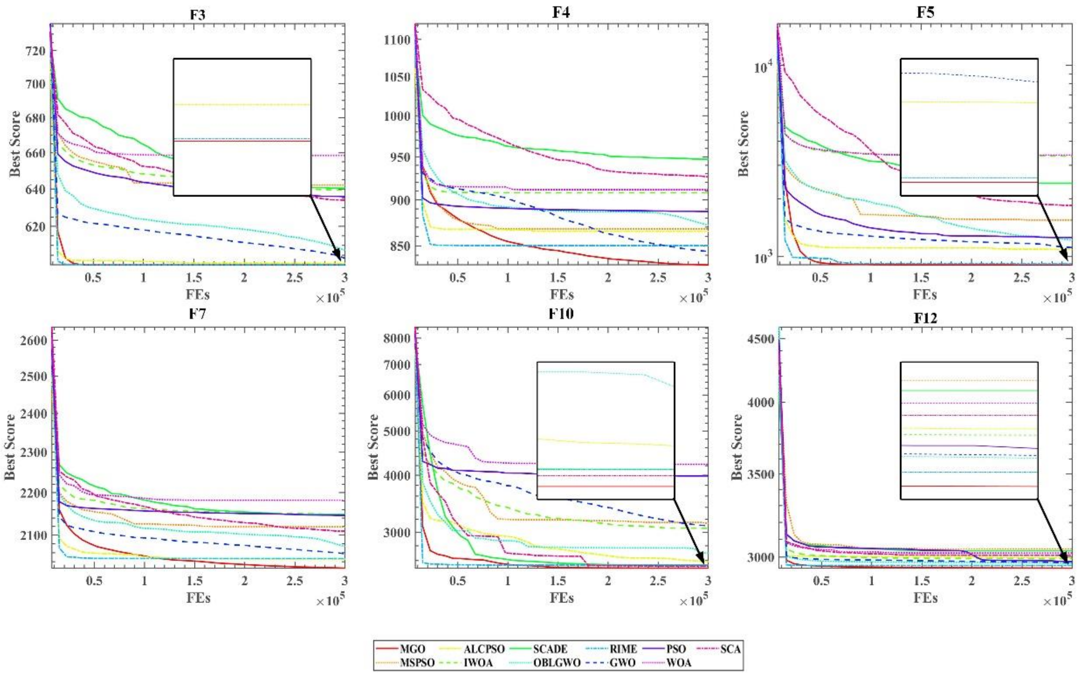

Figure 17. Convergence curves of MGO and other algorithms in CEC 2022.

3.3 Parameter sensitivity analysis

In this section, an evaluation was conducted on various values of key parameters to ascertain the optimal ones for MGO. Subsequently, a series of comparative experiments were undertaken on the various general parameters of MAs to find an appropriate problem size for MGO.

3.3.1 Analysis of critical parameters

In this section, this paper alters the parameters w in the equations Eq. (7) and Eq. (8), as elaborated in section 2.2.2. This adjustment is necessary because the parameter has a significant impact on spore dispersal search, which also plays a crucial role in MGO's global search capability—one of its noteworthy advantages. The experiment utilizes different values for the variable w, specifically 0.5, 1, 3, and 5, for comparison with the default value of 2. The comparison experiments are conducted within a standardized assessment framework, employing an equal number of populations, namely 30. And the dimension is set 30. The evaluations are carried out for a total of 300,000 evaluations, with the algorithm being independently parallelized in 30 instances. Furthermore, the CEC 2017 experimental test set is used as a benchmark for this evaluation.

More specifically, the variable w has an impact on the distance of spore dispersal both in $step1$ and $step2$. In Figure 18, the change in the first-dimensional value of $step1$ is depicted, where MGO_i denotes the value of w is set to i. As the iteration proceeds, the magnitude of $step1$ gradually diminishes, thereby indicating a gradual reduction in the extent of global exploration. Furthermore, a higher value of parameter w indicates a wider scope of the search; however, resulting in slower convergence of $step1$.

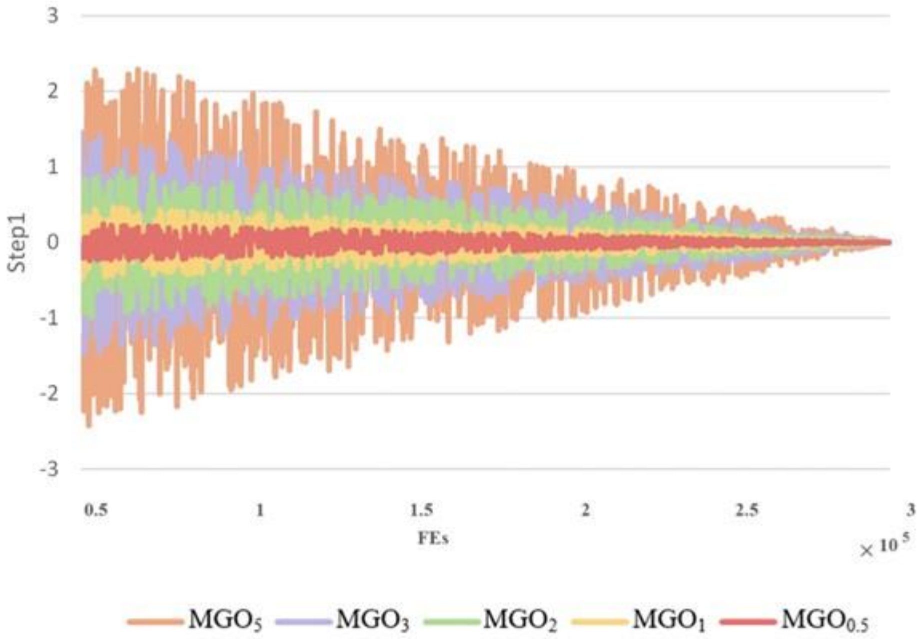

Figure 18. The first-dimensional value of *step*1 with different parameters.

Figure 19 illustrates the convergence curves of the five different parameters in the F5 function, providing a more intuitive understanding of the effects of various parameters w. As previously stated, when the value of w is increased, it leads to a broader range of search, which in turn causes a decrease in the speed of convergence. It is evident that MGO_5 took a significantly slower speed to reach convergence compared to $MGO_{0.5}$ during the initial stages. However, the final outcome of MGO_5 proved to be superior to that of $MGO_{0.5}$. It is important to note that a larger w does not guarantee a better result. In fact, it can be observed that MGO_3 achieved the best results.

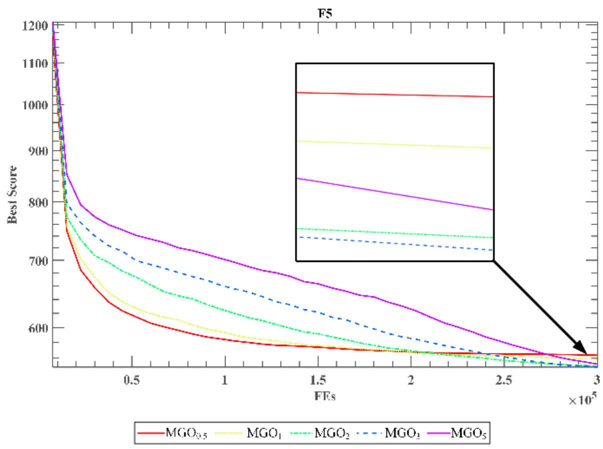

Figure 19. Convergence curves of different parameters w.

The algorithm's ranking for five different parameters is displayed in Table 8, where the Mean denotes the average value of the algorithm across all functions. MGO_3 achieved the highest mean score of 2.1724, indicating its superior overall performance. Despite having a lower Mean score than MGO3, MGO2 still ranked within the top three for all functions except F14. Moreover, Figure 20 provides the results of the FT analysis. It is evident that the analysis of MGO_2 from the FT perspective yielded superior results, with a value of 2.61. It is worth noting that although MGO_2 performed the best, overall, the difference in FT values was not significant, indicating MGO's insensitivity to parameters.

In actuality, it can be presumed that there is a minimal disparity between selecting 2 or 3. However, based on the aforementioned analysis, MGO_2 converges at a faster speed than MGO_3. Additionally, the search step is smaller, indicating that MGO_2 is more stable. Therefore, this paper will adopt MGO_2, which means set the value of w to 2. Researchers can select appropriate parameters based on the complexity of the problem and the number of iterations required. For simpler functions or fewer iterations, a smaller w parameter is suitable, whereas for more complex problems, a larger w parameter is recommended.

Table 8. Ranking of results with different values of parameter w.

Functions	$MGO_{0.5}$	MGO_1	MGO_2	MGO_3	MGO_5
F1	5	4	3	2	1
F3	3	1	2	4	5
F4	5	4	3	2	1
F5	5	4	2	1	3
F6	5	4	3	1	2
F7	5	4	2	1	3
F8	5	4	1	2	3
F9	5	4	2	1	3
F10	2	1	3	4	5
F11	5	4	2	1	3
F12	5	1	2	3	4
F13	5	1	2	4	3
F14	1	2	4	3	5
F15	4	1	2	3	5
F16	5	4	3	2	1
F17	4	3	2	1	5
F18	1	2	3	4	5
F19	5	1	2	3	4
F20	5	4	3	1	2
F21	5	4	3	2	1
F22	2	1	3	4	5
F23	5	4	2	1	3
F24	4	5	2	1	3
F25	5	4	3	1	2
F26	5	1	2	3	4
F27	5	2	3	1	4

F28	5	3	1	2	4
F29	4	1	3	2	5
F30	5	1	2	3	4
Mean	4.3103	2.7241	2.4137	2.1724	3.3793
Rank	5	3	2	1	4

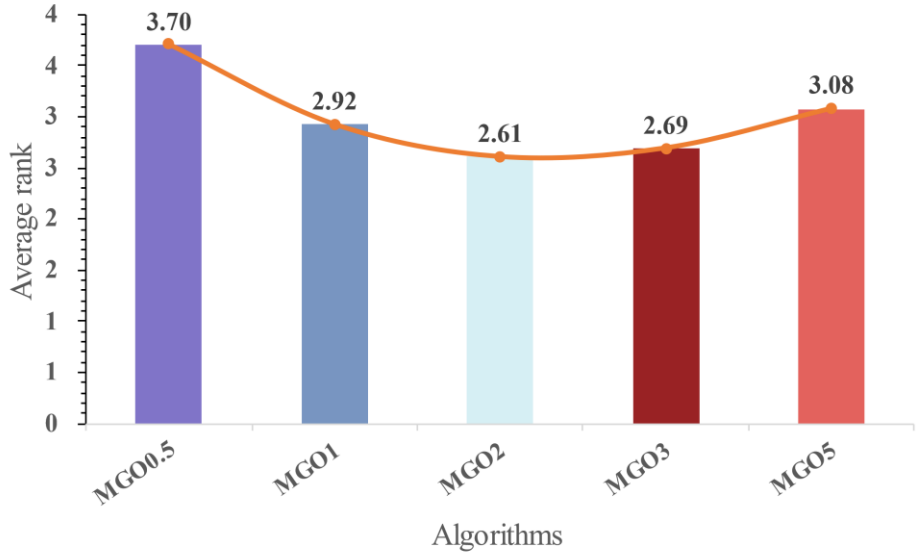

Figure 20. The average ranking of different parameters *w*.

3.3.2 Analysis of population size and number of iterations

For MAs, the optimization precision and efficiency of optimization problems are affected by population size and the number of iterations. It should be noted that, in this experiment, the operation is measured in terms of iterations, not evaluations. This is because the method of evaluation assesses the fitness of each individual in the function. As the population size increases, the number of evaluations used in each iteration also increases, decreasing the number of iterations. The relationship between iterations and evaluations can be seen in Eq. (14).

$$Fes = Its \cdot popSize \tag{14}$$

where Its denotes number of iterations, Fes denotes number of evaluations, and $popSize$ denotes population size.

To demonstrate the impact of population size on MAs, using iterations is clearly more effective, as it is not influenced by population size. The experimental population sizes were 5, 10, 30, 50, and 100, while the number of iterations varied at 1,000, 1,500, 2,000, 2,500, and 3,000. The dimension was set at 30, and each scenario was independently run 30 times, with the mean being calculated. The function used for testing is F6.

The test results are shown in Figure 21. It is apparent that as the size of Iterations increases, MGO always continuously seeks better solutions, regardless of the population size. Moreover, when Iterations is small, increasing the population size can effectively accelerate the convergence speed of the algorithm. However, after the population size exceeds 30, the additional effect becomes less apparent. In conclusion, the number of Iterations and the population size significantly impact MGO's search for optimal solutions and convergence speed.

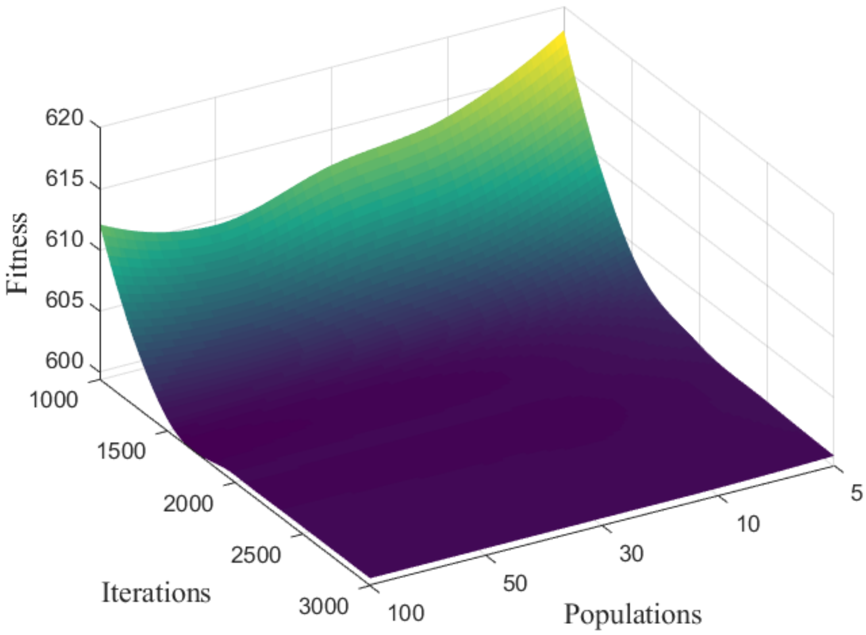

Figure 21. The influence of populations and iterations.

3.3.3 Analysis of dimension

In the calculation process of MGO, the mechanism for determining wind direction is based on the division of dimensions. Therefore, the number of dimensions of the problem is likely to significantly impact MGO. The experimental dimension consisted of 10, 30, 50, and 100 settings. The size of the population was 30, while the number of evaluations conducted reached 300,000. Each independent run was repeated a total of 30 times. The experiment was tested at CEC 2017.

Table A4 (Appendix) displays the Avg and Std in various dimensions of MGO. MGO10 represents MGO running in a 10-dimensional space, while the others exhibit similar characteristics. It is evident that MGO10 achieved the best results and demonstrated the highest level of stability. In order to further examine the impact of dimensions on MGO,

Figure 22 presents a comparison test using FT between MGO and other algorithms. These algorithms are the same as those discussed in section 3.2.1. As the dimensions increase, the advantage of MGO gradually diminishes, with MGO ranking second in 100 dimensions, surpassed by RIME. It is evident from this observation that MGO is better suited for resolving optimization problems of lower dimensions. In addition, when addressing practical issues, researches can consider adjusting the value of dn based on whether the population size is significantly smaller than the dimension, such as $\lfloor dim/8 \rfloor$, $\lfloor dim/16 \rfloor$, and so on.

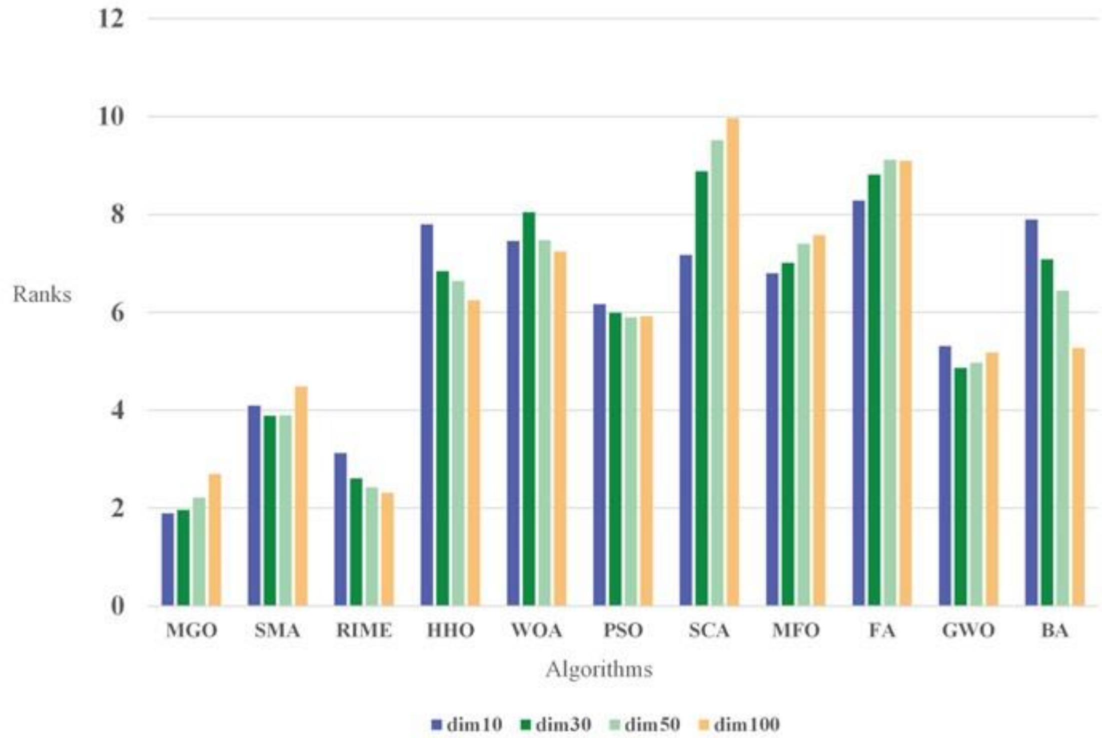

Figure 22. Friedman-rank of MGO and other algorithms in different dimensions.

3.4 Time spent analysis

The execution time of MAs is of great importance. In practice, this determines the efficiency of MAs when applied to real-world problems, especially for tasks with high real-time requirements, where MAs with faster execution times have a more significant advantage. In this section, the run times of MGO are compared with 10 original algorithms on 4 functions selected from the CEC 2017 test set. These functions are F1, F4, F11, and F21, respectively, corresponding to unimodal, multimodal, hybrid, and composition functions. All algorithms are executed under the same framework, with an equal number of populations of 30 and a dimension set to 30. The evaluations are conducted for a total of 300,000 evaluations, with the algorithm being independently parallelized in 30 instances. The specific method for calculating the spend time is to take the average of the times obtained from 30 independent runs. The measurement unit used is seconds.

The running times of all the algorithms can be observed in Figure 23. It is evident that the WOA algorithm has the shortest total running time, followed by PSO, while the total running time of SMA is considerably higher than that of other algorithms. The running time details are specified in Table 9. The MGO's runtime is only marginally slower than that of the WOA by less than a second, a discrepancy that can be deemed permissible.

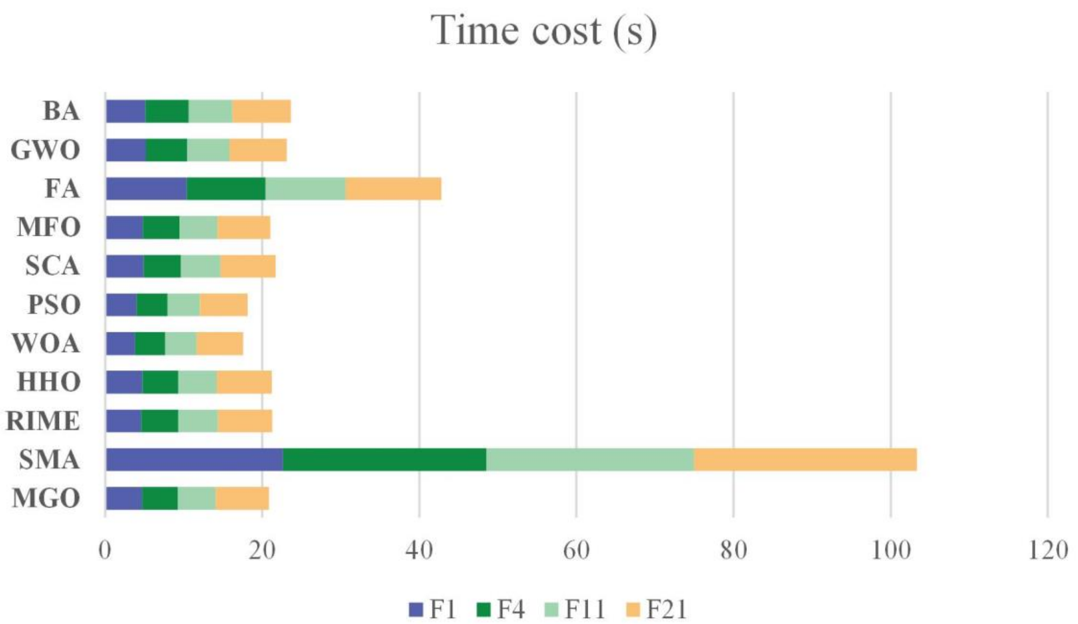

Figure 23. Total running time of each algorithm.

Table 9. Running time of MGO and other algorithms.

Algorithms	F1	F4	F11	F21
MGO	4.712E+00	4.571E+00	4.763E+00	6.812E+00
SMA	2.263E+01	2.592E+01	2.642E+01	2.836E+01
RIME	4.565E+00	4.774E+00	5.011E+00	6.941E+00
HHO	4.756E+00	4.555E+00	4.890E+00	7.009E+00
WOA	3.832E+00	3.808E+00	4.010E+00	5.916E+00
PSO	4.000E+00	3.942E+00	4.148E+00	6.051E+00
SCA	4.887E+00	4.781E+00	5.029E+00	6.989E+00
MFO	4.825E+00	4.658E+00	4.828E+00	6.737E+00
FA	1.040E+01	1.001E+01	1.021E+01	1.221E+01
GWO	5.214E+00	5.238E+00	5.357E+00	7.323E+00
BA	5.153E+00	5.474E+00	5.551E+00	7.481E+00

3.5 Time spent analysis

When compared to gradient-based methods, MAs offer significant benefits in terms of shape and structural optimization (Richards & Amos, 2016). They are particularly well-suited for handling complex, multimodal design spaces and highly nonlinear objective functions. Moreover, their user-friendly characteristics make them suitable for both designers and non-specialist engineers. However, it should be noted that a particular algorithm may not be suitable for all optimization problems (Wolpert & Macready, 1997). This is why it is necessary to constantly propose novel algorithms and validate their applicability in specific domains.

This section applies MGO to 4 engineering optimization problems. Engineering optimization problems refer to the use of specific techniques to find the most cost-effective and efficient solution for a problem or design in the field of engineering. The complex and highly constrained nature of engineering optimization problems presents a greater challenge for algorithms to resolve (Zhao et al., 2023). The algorithms employed for comparison include BA(Yang, 2010), Cuckoo search algorithm (CS) (Gandomi et al., 2013), GWO (Mirjalili et al., 2014), MFO (Mirjalili, 2015), opposition-based sine cosine algorithm (OBSCA) (Abd Elaziz et al., 2017), RIME (Su et al., 2023). For all experiments, the population size is fixed at 50, and the iteration count is set to 2000. Each algorithm is independently run 50 times to obtain optimal solutions, which are then used as the basis for the results.

3.5.1 Pressure vessel design problem

The pressure vessel design (Mirjalili, 2015) is a problem of engineering optimization, with the objective of assessing the most suitable thickness for the shell T_s, the thickness of the head T_h, the inner radius R, and the length of the shell, denoted as L. These parameters are determined in order to minimize the overall cost of material, forming, and welding, taking into consideration four specific constraints. It is worth noting that T_s and T_h are values expressed as integer multiples of 0.0625 in., which represent the available thicknesses of rolled steel plates, while R and L are continuous variables. Figure 24 depicts the structure of the pressure vessel design. The subsequent is the mathematical representation of the problem.

Consider:

$$X = [x_1, x_2, x_3, x_4] = [T_s, T_h, R, L]$$

Objective:

$$\min f(X) = 0.6224x_1x_3x_4 + 1.7781x_2x_3^2 + 3.1661x_1^2x_4 + 19.84x_1^2x_3$$

Subject to:

$$g_1 = -x_1 + 0.0193x_3 \le 0$$
$$g_2 = -x_2 + 0.00954x_3 \le 0$$
$$g_3 = -\pi x_3^2 x_4 - \frac{4}{3}\pi x_3^3 + 1296000 \le 0$$
$$g_4 = x_4 - 240 \le 0$$

Variable ranges:

$$0.0625 \le x_1, x_2 \le 99 \cdot 0.0625$$
$$10 \le x_3, x_4 \le 200$$

As evidenced by the data presented in Table 10, while MGO did not attain the minimum thresholds for every parameter, it yielded the most economical outcome regarding pressure vessel design. This demonstrates the benefits and advantages with the utilization of MGO.

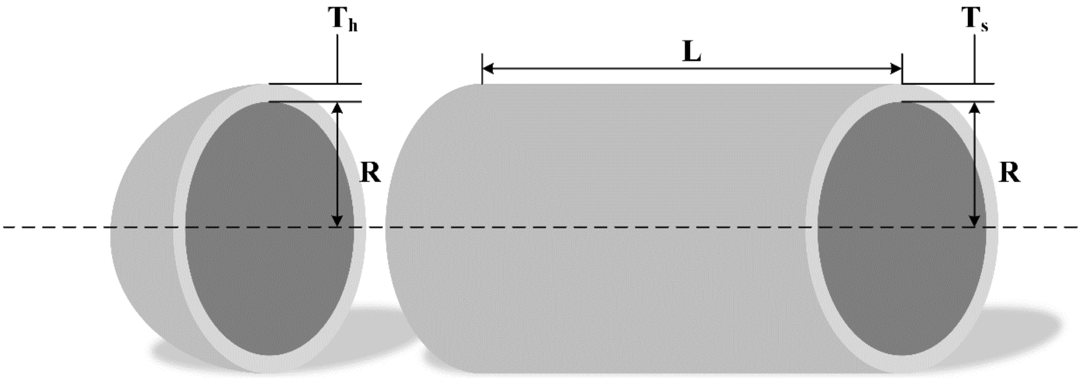

Figure 24. Structure of pressure vessel design.

Table 10. Comparison results of pressure vessel design problem.

Algorithms	Optimum variables				Optimum cost
	T_s	T_h	R	L	
MGO	**0.81250**	**0.43750**	42.09771	176.64590	**6059.80750**
BA	4.37500	0.62500	199.49998	200.00000	7379.01568
CS	1.12500	0.56250	55.78959	**58.35895**	6071.65500
GWO	**0.81250**	**0.43750**	42.09784	176.64538	6059.81846
MFO	1.00000	0.50000	51.58740	85.72137	6433.88664
OBSCA	0.87500	0.62500	42.40156	200.00000	7745.28645
RIME	**0.81250**	**0.43750**	**42.09169**	176.72436	6060.63089

3.5.2 Welded beam design problem

The welded beam design problem (Li et al., 2020) is to ascertain the welded beam that has the least expensive cost, taking into account four limitations and the key characteristics of shear stress τ, bending stress θ, buckling load P_c, and deflection δ. As depicted in Figure 25, this task encompasses the four variables: the thickness of the welding seam h, the length of the welding joint l, the width of the beam t, and the thickness of the beam b. The subsequent content presents the mathematical model for this problem.

Consider:

$$X = [x_1, x_2, x_3, x_4] = [h, l, t, b]$$

Objective:

$$\min f(X) = 1.10471 x_1^2 x_2 + 0.04811 x_3 x_4 (14 + x_2)$$

Subject to:

$$\begin{gathered} g_1(X) = \tau(X) - \tau_{max} \leq 0 \\ g_2(X) = \sigma(X) - \sigma_{max} \leq 0 \\ g_3(X) = \delta(X) - \delta_{\max} \leq 0 \\ g_4(X) = x_1 - x_4 \leq 0 \\ g_5(X) = P - P_C(X) \leq 0 \\ g_6(X) = 0.125 - x_1 \leq 0 \\ g_7(X) = 1.10471 x_1^2 + 0.04811 x_3 x_4 (14.0 + x_2) - 5.0 \leq 0 \end{gathered}$$

Variable ranges:

$$\begin{gathered} 0.1 \leq x_1, x_4 \leq 2 \\ 0.1 \leq x_2, x_3 \leq 10 \end{gathered}$$

where

$$\tau(X) = \sqrt{(\tau')^2 + 2\tau'\tau''\frac{x_2}{2R} + (\tau'')^2}$$
$$\tau' = \frac{P}{\sqrt{2}x_1x_2}, \tau'' = \frac{MR}{J}, M = P(L + x_2/2)$$
$$R = \sqrt{\frac{x_2^2}{4} + \frac{(x_1 + x_3)^2}{4}}$$
$$J = 2\{\frac{x_1x_2}{\sqrt{2}}[\frac{x_2^2}{12} + \left(\frac{x_1 + x_3}{2}\right)^2]\}$$
$$\sigma(X) = \frac{6PL}{x_4x_3^2}, \delta(\vec{x}) = \frac{4PL^3}{Ex_3^3x_4}$$
$$P_c(\vec{x}) = \frac{4.013\sqrt{E\frac{Gx_3^2x_4^6}{36}}}{L^2}(1 - \frac{x_3}{2L}\sqrt{\frac{E}{4G}})$$
$$P = 6000\text{lb}, L = 14\text{in}, E = 30 \times 10^6\text{psi}, G = 12 \times 10^6\text{psi}$$
$$\tau_{\max} = 13{,}600 \text{ psi}, \sigma_{max} = 30{,}000 \text{ psi}, \delta_{max} = 0.25 \text{ in}$$

According to the data presented in Table 11, it is evident that MGO achieved superior outcomes in comparison to the other algorithms.

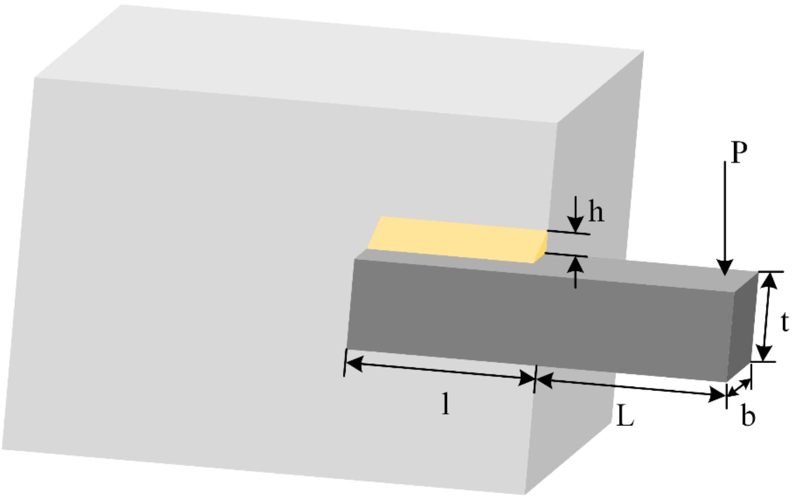

Figure 25. Structure of welded beam design.

Table 11. Comparison results of welded beam design problem.

Algorithms	Optimum variables				Optimum cost
	h	l	t	b	
MGO	0.20572	3.47099	9.03609	0.20575	**1.72499**
BA	2.0	10.0	**1.0**	**0.1**	1.93349

	0000	0000	**1979**	**0000**	
CS	**0.19916**	5.30471	7.10414	0.34582	1.72812
GWO	0.20571	3.47111	9.03749	0.20573	1.72503
MFO	0.20178	3.51587	9.28318	0.20473	1.75968
OBSCA	0.22858	**3.46404**	8.19220	0.26376	2.01542
RIME	0.20547	3.47370	9.04552	0.20575	1.72658

3.5.3 Three-bar truss design problem

The three-bar truss design (Pathak & Srivastava, 2022) is a problem of engineering optimization, aiming to assess the optimal cross-sectional areas $A_1 = A_3$ and A_2 in order to minimize the volume of the truss structure under static loading, while considering stress σ restrictions. Figure 26 illustrates the proportions of the three-bar truss construction. The subsequent content presents the mathematical model for this problem.

Consider:

$$X = [x_1, x_2] = [A_1/A_3, A_2]$$

Objective:

$$min f(X) = (2\sqrt{2}x_1 + x_2) \times H$$

Subject to:

$$g_1 = \frac{\sqrt{2}x_1 + x_2}{\sqrt{2}x_1^2 + 2x_1x_2} P - \sigma \leq 0$$
$$g_2 = \frac{x_2}{\sqrt{2}x_1^2 + 2x_1x_2} P - \sigma \leq 0$$
$$g_3 = \frac{1}{x_1 + \sqrt{2}x_2} P - \sigma \leq 0$$

Variable ranges:

$$0 \leq x_1, x_2 \leq 1$$

where

$$H = 100cm$$
$$P = 2KN/cm^2$$
$$\sigma = 2KN/cm^2$$

As is evident from the data presented in Table 12, it is apparent that MGO exhibited the most favorable outcomes when compared to all other algorithms under consideration.

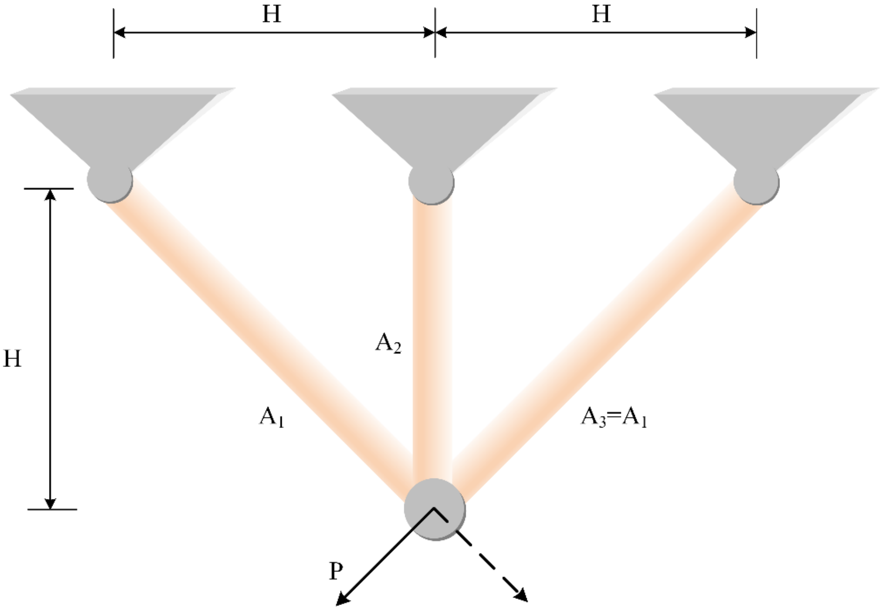

Figure 26. Structure of three-bar truss design.

Table 12. Comparison results of three-bar truss design.

Algorithms	Optimum variables		Optimum cost
	A_1/A_3	A_2	
MGO	0.78870	0.40818	**263.89586**
BA	**0.14753**	1.00000	263.96253
CS	0.78858	0.40853	263.89605
GWO	0.78903	0.40725	263.89599
MFO	0.79005	**0.40471**	263.92972
OBSCA	0.78928	0.40974	264.21740
RIME	0.78867	0.40827	**263.89586**

3.5.4 Speed reducer design problem

A speed reducer is an integral component of the mechanical system's gear box and finds application in various other contexts (Hassan et al., 2005). Figure 27 depicts the structure of the speed reducer design. The design of the speed reducer poses a more formidable benchmark, taking into account parameters such as the face width b, the module of the teeth

m, the number of teeth on the pinion p, the length of the first shaft between the bearings l_1, the length of the second shaft between the bearings l_2, the diameter of the first shaft d_1, and the diameter of the second shaft d_2. The subsequent content presents the mathematical model for this problem.

Consider:

$$X = [x_1, x_2, x_3, x_4, x_5, x_6, x_7] = [b, m, p, l_1, l_2, d_1, d_2]$$

Objective:

$$\begin{aligned} minf(X) = 0.7854x_1x_2^2(3.3333x_3^2 + 14.9334x_3 - 43.0934) \\ - 1.508x_1(x_6^2 + x_7^2) + 7.4777(x_6^3 + x_7^3) + 0.7854(x_4x_6^2 + x_5x_7^2) \end{aligned}$$

Subject to:

$$g_1 = 27x_1^{-1}x_2^{-2}x_3^{-1} - 1 \leq 0$$
$$g_2 = 397.5x_1^{-1}x_2^{-2}x_3^{-2} - 1 \leq 0$$
$$g_3 = 1.93x_4^3x_2^{-1}x_3^{-1}x_6^{-4} - 1 \leq 0$$
$$g_4 = 1.93x_5^3x_2^{-1}x_3^{-1}x_7^{-4} - 1 \leq 0$$
$$g_5 = \frac{1}{110x_6^3}\sqrt{(\frac{745x_4}{x_2x_3})^2 + 16.9 \times 10^6} - 1 \leq 0$$
$$g_6 = \frac{1}{85x_7^3}\sqrt{(\frac{745x_5}{x_2x_3})^2 + 157.5 \times 10^6} - 1 \leq 0$$
$$g_7 = x_2x_3 - 40 \leq 0$$
$$g_8 = 5x_2 - x_1 \leq 0$$
$$g_9 = x_1 - 12x_2 \leq 0$$
$$g_{10} = 1.5x_6 - x_4 + 1.9 \leq 0$$
$$g_{11} = 1.1x_7 - x_5 + 1.9 \leq 0$$

Variable ranges:

$$2.6 \leq x_1 \leq 3.6$$
$$0.7 \leq x_2 \leq 0.8$$
$$17 \leq x_3 \leq 28$$
$$7.3 \leq x_4, x_5 \leq 8.3$$
$$2.9 \leq x_6 \leq 3.9$$
$$5 \leq x_7 \leq 5.5$$

Table 13 presents the empirical findings. Evidently, MGO attained minimal values for the majority of parameters, ultimately yielding optimal outcomes.

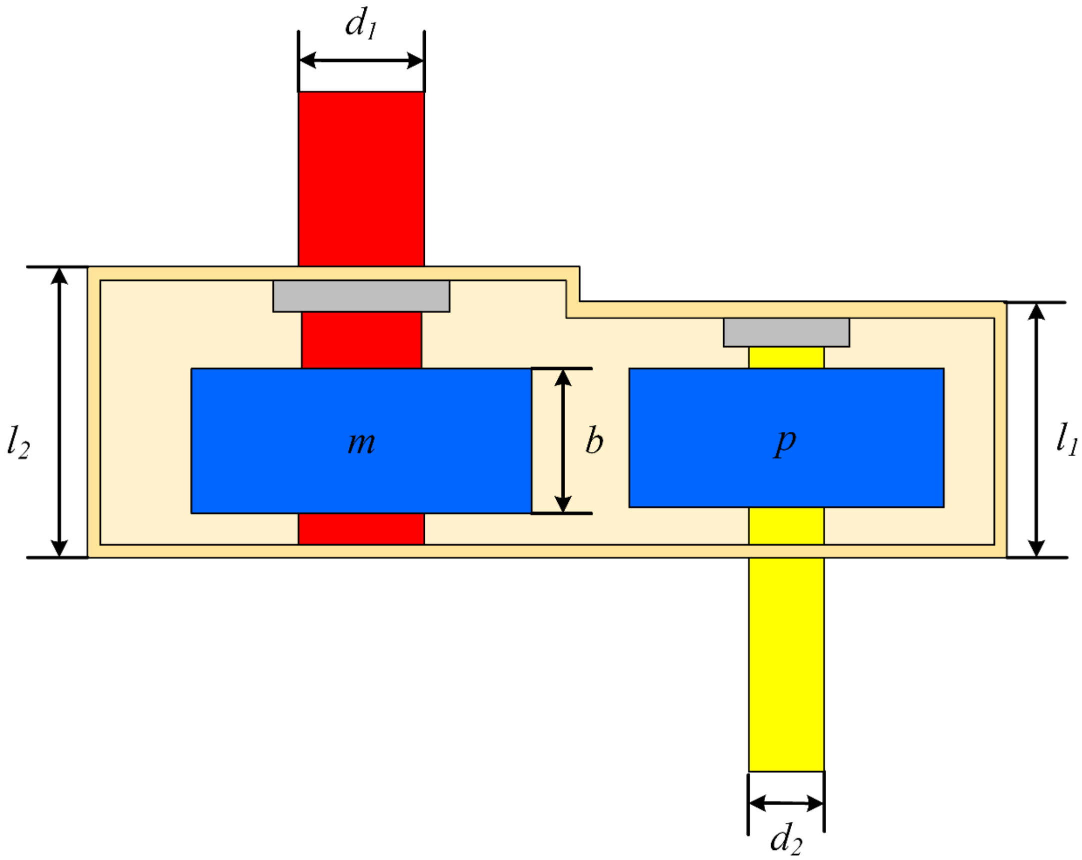

Figure 27. Structure of speed reducer design.

Table 13. Comparison results of speed reducer design problem.

Algorithms	Optimum variables							Optimum cost
	b	m	p	l_1	l_2	d_1	d_2	
MGO	**3.500**	0.700	17.000	**7.300**	7.715	**3.350**	**5.287**	**2994.477**
BA	3.600	0.700	17.000	**7.300**	**7.300**	3.605	5.380	3028.489
CS	**3.500**	0.700	17.000	**7.300**	7.720	**3.350**	**5.287**	2994.962
GWO	3.501	0.700	17.000	7.484	7.763	3.353	**5.287**	2998.595
MFO	3.502	0.700	17.000	7.370	7.751	3.351	5.293	3001.108

OBSCA	3.600	0.700	17.000	8.300	8.300	3.615	5.353	3172.114
RIME	**3.500**	0.700	17.000	**7.300**	7.716	**3.350**	**5.287**	2994.511

4. Conclusions and future works

In this study, a useful optimization algorithm was proposed, drawing inspiration from the growth phenomenon observed in moss to resolve intricate optimization problems. The MGO algorithm initially introduced the method of determination of wind direction to determine the direction of the wind, that is, the overall evolution direction of the population. Based on this, the method of spore dispersal search was proposed, which was inspired by the spore dispersal of moss, and it uses two different steps to change the current individual. Then, the dual propagation search, inspired by the sexual and vegetative moss reproduction, was proposed, including two individual updating strategies. Lastly, the cryptobiosis mechanism was proposed, which improves the greedy selection mechanism and prevents the algorithm from falling into local optima. In the experimental section, the qualitative analysis was initially established for MGO, showcasing the distribution of past searches, the individual trajectory, the population's fitness, and the convergence curve. This analysis demonstrated the effective global search capability of MGO but also revealed its relatively slow convergence. Subsequently, a benchmark test was conducted at CEC 2017, wherein a comparison was made between 10 original algorithms and 10 advanced algorithms. The final results were compared using Avg and Std, in addition to conducting WSRT and FT analyses on the results and presenting the convergence curves of the algorithms. These findings demonstrate that MGO exhibits highly promising performance and outperforms its competitors in the majority of benchmark functions. CEC 2022 benchmark tests were conducted, demonstrating that MGO's advantages extend beyond CEC 2017. This paper discusses the optimal parameters and suitable problem scales for MGO through parameter sensitivity analysis. The time spent analysis confirmed that the runtime of MGO falls within an acceptable range. Ultimately, the successful deployment of the MGO algorithm in engineering design problems underscores its proficiency in addressing sophisticated optimization challenges. Notably, the algorithm's performance is particularly commendable under conditions where the number of iterations is constrained, yet it consistently delivers robust solutions. This achievement can be attributed to the adaptive ability inherent in MGO, which facilitates a self-regulating adjustment process that aligns seamlessly with the nuances of the problem at hand. The responsive nature of these mechanisms is instrumental in navigating the intricate dynamics of complex optimization scenarios, thereby reinforcing the algorithm's utility and relevance in engineering optimization.

The previously mentioned experiments offer concrete evidence of the benefits of MGO. These achievements can be attributed to several key factors:

1. The spore dispersal search strategy enables the majority of individuals to direct their search toward the optimal individuals, whereas the remaining individuals can engage in thorough exploration.
2. Benefitting from the two steps of spore dispersal search, MGO algorithm tends towards a higher degree of exploration and a lower degree of exploitation in the initial phase, which gradually transforms into a lower degree of exploration and a higher degree of exploitation as the step length decreases. This approach effectively balances the exploration and exploitation aspects of each stage.
3. Dual propagation search enhances the accuracy and efficiency of finding optimal solutions by selectively replicating and propagating components from the optimal solution.
4. The cryptobiosis mechanism abandons the direct alteration of individuals for updating and instead updates current individuals based on recorded information. This approach is beneficial in preventing algorithms from falling into local optimal solutions.

Although the MGO algorithm has shown outstanding performance in various tests and applications, it still has some limitations. One primary limitation is that MGO's convergence is slow, which may put it at a disadvantage when dealing with problems that require fewer iterations. Additionally, the algorithm may experience performance degradation when dealing with high-dimensional search spaces. Moreover, for specific optimization problems, such as those with multiple local optima, MGO may require further adjustments to improve its performance. Integrating MGO with specific mechanisms could potentially resolve the issues mentioned in the future. Additionally, it would be beneficial to focus on exploring binary and multi-objective variations of MGO, particularly in real-world problem-solving. Future studies may also enhance the MGO algorithm to manage high-dimensional problems effectively. In parallel, there is an opportunity for researchers to develop hybrid MGO algorithms that incorporate other optimization strategies, aiming to improve their performance on particular cases.

Conflicts of interest

The authors declare no conflict of interest.

Author contributions

Boli Zheng: Writing – Original Draft; Yi Chen: Formal Analysis and Investigation; Chaofan Wang: Resource; Ali Asghar Heidari: Writing – Review & Editing and Funding acquisition; Lei Liu: Resource; Huiling Chen: Funding acquisition.

Data availability

The data involved in this study are all public data, which can be downloaded through public channels.

References

Abd Elaziz, M., Oliva, D., & Xiong, S. (2017). An improved opposition-based sine cosine algorithm for global optimization. *Expert Systems with Applications*, *90*, 484-500.

Abdel-Basset, M., Mohamed, R., Jameel, M., & Abouhawwash, M. (2023). Spider wasp optimizer: A novel meta-heuristic optimization algorithm. *Artificial Intelligence Review*, *56*(10), 11675-11738.

Ahrari, A., Elsayed, S., Sarker, R., Essam, D., & Coello, C. (2022). Problem Definition and Evaluation Criteria for the CEC'2022 Competition on Dynamic Multimodal Optimization. https://doi.org/10.13140/rg.2.2.32347.85284

Alcalá-Fdez, J., Sanchez, L., Garcia, S., del Jesus, M. J., Ventura, S., Garrell, J. M., Otero, J., Romero, C., Bacardit, J., & Rivas, V. M. (2009). KEEL: a software tool to assess evolutionary algorithms for data mining problems. *Soft Computing*, *13*, 307-318.

Asif, S., Zhao, M., Tang, F., Zhu, Y., & Zhao, B. (2023). Metaheuristics optimization-based ensemble of deep neural networks for Mpox disease detection. *Neural Networks*, *167*, 342-359.

Beyer, H.-G., & Schwefel, H.-P. (2002). Evolution strategies–a comprehensive introduction. *Natural computing*, *1*, 3-52.

Bouaouda, A., & Sayouti, Y. (2022). Hybrid meta-heuristic algorithms for optimal sizing of hybrid renewable energy system: a review of the state-of-the-art. *Archives of Computational Methods in Engineering*, *29*(6), 4049-4083.

Cannone, N., Corinti, T., Malfasi, F., Gerola, P., Vianelli, A., Vanetti, I., Zaccara, S., Convey, P., & Guglielmin, M. (2017). Moss survival through in situ cryptobiosis after six centuries of glacier burial. *Scientific Reports*, *7*(1), 4438.

Cao, B., Gu, Y., Lv, Z., Yang, S., Zhao, J., & Li, Y. (2021). RFID Reader Anticollision Based on Distributed Parallel Particle Swarm Optimization. *IEEE Internet of Things Journal*, *8*(5), 3099-3107. https://doi.org/10.1109/JIOT.2020.3033473

Cao, B., Wang, X., Zhang, W., Song, H., & Lv, Z. (2020). A Many-Objective Optimization Model of Industrial Internet of Things Based on Private Blockchain. *IEEE Network*, *34*(5), 78-83.

Cao, B., Zhang, W., Wang, X., Zhao, J., Gu, Y., & Zhang, Y. (2021). A memetic algorithm based on two_Arch2 for multi-depot heterogeneous-vehicle capacitated Arc routing problem. *Swarm and Evolutionary Computation*, *63*, 100864.

Cao, B., Zhao, J., Gu, Y., Ling, Y., & Ma, X. (2020). Applying graph-based differential grouping for multiobjective large-scale optimization. *Swarm and Evolutionary Computation*, *53*, 100626.

Cao, B., Zhao, J., Yang, P., Gu, Y., Muhammad, K., Rodrigues, J. J., & de Albuquerque, V. H. C. (2019). Multiobjective 3-D topology optimization of next-generation wireless data center network. *IEEE Transactions on Industrial Informatics*, *16*(5), 3597-3605.

Chen, H., Yang, C., Heidari, A. A., & Zhao, X. (2020). An efficient double adaptive random spare reinforced whale optimization algorithm. *Expert Systems with Applications*, *154*, 113018.

Chen, W.-N., Zhang, J., Lin, Y., Chen, N., Zhan, Z.-H., Chung, H. S.-H., Li, Y., & Shi, Y.-H. (2012). Particle swarm optimization with an aging leader and challengers. *IEEE Transactions on Evolutionary Computation*, *17*(2), 241-258.

Cove, D. (2005). The moss Physcomitrella patens. *Annu. Rev. Genet.*, *39*, 339-358.

Dehghani, M., Montazeri, Z., Trojovská, E., & Trojovský, P. (2023). Coati Optimization Algorithm: A new bio-inspired metaheuristic algorithm for solving optimization problems. *Knowledge-Based Systems*, *259*, 110011.

Duan, S., Jiang, S., Dai, H., Wang, L., & He, Z. (2023). The applications of hybrid approach combining exact method and evolutionary algorithm in combinatorial optimization. *Journal of Computational Design and Engineering*, *10*(3), 934-946.

Duan, Y., Zhao, Y., & Hu, J. (2023). An initialization-free distributed algorithm for dynamic economic dispatch problems in microgrid: Modeling, optimization and analysis. *Sustainable Energy, Grids and Networks*, 101004.

El-kenawy, E.-S. M., Khodadadi, N., Mirjalili, S., Abdelhamid, A. A., Eid, M. M., & Ibrahim, A. (2024). Greylag goose optimization: Nature-inspired optimization algorithm. *Expert Systems with Applications*, *238*, 122147.

Emam, M. M., Samee, N. A., Jamjoom, M. M., & Houssein, E. H. (2023). Optimized deep learning architecture for brain tumor classification using improved Hunger Games Search Algorithm. *Comput Biol Med*, *160*, 106966.

Ferahtia, S., Rezk, H., Djerioui, A., Houari, A., Motahhir, S., & Zeghlache, S. (2023). Modified bald eagle search algorithm for lithium-ion battery model parameters extraction. *ISA transactions*, *134*, 357-379.

Gandomi, A. H., Yang, X.-S., & Alavi, A. H. (2013). Cuckoo search algorithm: a metaheuristic approach to solve structural optimization problems. *Engineering with Computers*, *29*, 17-35.

Geem, Z. W., Kim, J. H., & Loganathan, G. V. (2001). A new heuristic optimization algorithm: harmony search. *simulation*, *76*(2), 60-68.

Ghorbani, N., & Babaei, E. (2014). Exchange market algorithm. *Applied Soft Computing*, *19*, 177-187.

Guo, H., Li, M., Liu, H., Chen, X., Cheng, Z., Li, X., Yu, H., & He, Q. (2024). Multi-threshold Image Segmentation based on an improved Salp Swarm Algorithm: Case study of breast cancer pathology images. *Comput Biol Med*, *168*, 107769.

Hansen, N., & Ostermeier, A. (2001). Completely derandomized self-adaptation in evolution strategies. *Evolutionary computation*, *9*(2), 159-195.

Hao, S., Huang, C., Heidari, A. A., Chen, H., Li, L., Algarni, A. D., Elmannai, H., & Xu, S. (2023). Salp swarm algorithm with iterative mapping and local escaping for multi-level threshold image segmentation: A skin cancer dermoscopic case study. *Journal of Computational Design and Engineering*, *10*(2), 655-693.

Hassan, R., Cohanim, B., De Weck, O., & Venter, G. (2005). A comparison of particle swarm optimization and the genetic algorithm. 46th AIAA/ASME/ASCE/AHS/ASC structures, structural dynamics and materials conference,

He, S., Wu, Q. H., & Saunders, J. R. (2009). Group search optimizer: an optimization algorithm inspired by animal searching behavior. *IEEE Transactions on Evolutionary Computation*, *13*(5), 973-990.

Heckman, D. S., Geiser, D. M., Eidell, B. R., Stauffer, R. L., Kardos, N. L., & Hedges, S. B. (2001). Molecular evidence for the early colonization of land by fungi and plants. *science*, *293*(5532), 1129-1133.

Heidari, A. A., Abbaspour, R. A., & Chen, H. (2019). Efficient boosted grey wolf optimizers for global search and kernel extreme learning machine training. *Applied Soft Computing*, *81*, 105521.

Heidari, A. A., Mirjalili, S., Faris, H., Aljarah, I., Mafarja, M., & Chen, H. (2019). Harris hawks optimization: Algorithm and applications. *Future Generation Computer Systems*, *97*, 849-872. https://doi.org/https://doi.org/10.1016/j.future.2019.02.028

Holland, J. H. (1992). Genetic algorithms. *Scientific american*, *267*(1), 66-73.

Hussein, N. K., Qaraad, M., Amjad, S., Farag, M., Hassan, S., Mirjalili, S., & Elhosseini, M. A. (2023). Enhancing feature selection with GMSMFO: A global optimization algorithm for machine learning with application to intrusion detection. *Journal of Computational Design and Engineering*, *10*(4), 1363-1389.

Irizarry, R. (2004). LARES: an artificial chemical process approach for optimization. *Evolutionary computation*, *12*(4), 435-459.

Jaafari, A., Termeh, S. V. R., & Bui, D. T. (2019). Genetic and firefly metaheuristic algorithms for an optimized neuro-fuzzy prediction modeling of wildfire probability. *Journal of environmental management*, *243*, 358-369.

Javidy, B., Hatamlou, A., & Mirjalili, S. (2015). Ions motion algorithm for solving optimization problems. *Applied Soft Computing*, *32*, 72-79.

Jia, H., & Lu, C. (2024). Guided learning strategy: A novel update mechanism for metaheuristic algorithms design and improvement. *Knowledge-Based Systems*, *286*, 111402.

Johansson, V., Lönnell, N., Rannik, Ü., Sundberg, S., & Hylander, K. (2016). Air humidity thresholds trigger active moss spore release to extend dispersal in space and time. *Functional Ecology*, *30*(7), 1196-1204.

Johnson, M., & Shaw, A. (2016). The effects of quantitative fecundity in the haploid stage on reproductive success and diploid fitness in the aquatic peat moss Sphagnum macrophyllum. *Heredity*, *116*(6), 523-530.

Karaboga, D. (2005). *An idea based on honey bee swarm for numerical optimization*.

Kaveh, A., & Dadras, A. (2017). A novel meta-heuristic optimization algorithm: thermal exchange optimization. *Advances in engineering software*, *110*, 69-84.

Kennedy, J., & Eberhart, R. (1995). Particle swarm optimization. Proceedings of ICNN'95-international conference on neural networks,

Kirkpatrick, S., Gelatt Jr, C. D., & Vecchi, M. P. (1983). Optimization by simulated annealing. *science*, *220*(4598), 671-680.

Koza, J. R. (1994). Genetic programming as a means for programming computers by natural selection. *Statistics and computing*, *4*, 87-112.

Kumar, N., Hussain, I., Singh, B., & Panigrahi, B. K. (2017). Single sensor-based MPPT of partially shaded PV system for battery charging by using cauchy and gaussian sine cosine optimization. *IEEE Transactions on Energy Conversion*, *32*(3), 983-992.

Kundu, R., & Mallipeddi, R. (2022). HFMOEA: A hybrid framework for multi-objective feature selection. *Journal of Computational Design and Engineering*, *9*(3), 949-965.

Li, S., Chen, H., Wang, M., Heidari, A. A., & Mirjalili, S. (2020). Slime mould algorithm: A new method for stochastic optimization. *Future Generation Computer Systems*, *111*, 300-323. https://doi.org/https://doi.org/10.1016/j.future.2020.03.055

Li, X., Lin, Z., Lv, H., Yu, L., Heidari, A. A., Zhang, Y., Chen, H., & Liang, G. (2023). Advanced slime mould algorithm incorporating differential evolution and Powell mechanism for engineering design. *iScience*, *26*(10), 107736.

Lian, J., & Hui, G. (2024). Human evolutionary optimization algorithm. *Expert Systems with Applications*, *241*, 122638.

Liang, H., Liu, Y., Shen, Y., Li, F., & Man, Y. (2018). A hybrid bat algorithm for economic dispatch with random wind power. *IEEE Transactions on Power Systems*, *33*(5), 5052-5061.

Lueth, V. M., & Reski, R. (2023). Mosses. *Current Biology*, *33*(22), R1175-R1181.

Luo, J., Zhuo, W., Liu, S., & Xu, B. (2024). The Optimization of Carbon Emission Prediction in Low Carbon Energy Economy Under Big Data. *IEEE Access*, *12*, 14690-14702. https://doi.org/10.1109/ACCESS.2024.3351468

Matoušová, I., Trojovský, P., Dehghani, M., Trojovská, E., & Kostra, J. (2023). Mother optimization algorithm: A new human-based metaheuristic approach for solving engineering optimization. *Scientific Reports*, *13*(1), 10312.

Meola, A., Winkler, M., & Weinrich, S. (2023). Metaheuristic optimization of data preparation and machine learning hyperparameters for prediction of dynamic methane production. *Bioresource Technology*, *372*, 128604.

Mirjalili, S. (2015). Moth-flame optimization algorithm: A novel nature-inspired heuristic paradigm. *Knowledge-Based Systems*, *89*, 228-249.

Mirjalili, S. (2016). SCA: a sine cosine algorithm for solving optimization problems. *Knowledge-Based Systems*, *96*, 120-133.

Mirjalili, S., & Lewis, A. (2016). The Whale Optimization Algorithm. *Advances in Engineering Software*, *95*, 51-67. https://doi.org/10.1016/j.advengsoft.2016.01.008
Mirjalili, S., Mirjalili, S. M., & Lewis, A. (2014). Grey wolf optimizer. *Advances in engineering software*, *69*, 46-61.
Nenavath, H., & Jatoth, R. K. (2018). Hybridizing sine cosine algorithm with differential evolution for global optimization and object tracking. *Applied Soft Computing*, *62*, 1019-1043.
Ngo, N.-T., Truong, T. T. H., Truong, N.-S., Pham, A.-D., Huynh, N.-T., Pham, T. M., & Pham, V. H. S. (2022). Proposing a hybrid metaheuristic optimization algorithm and machine learning model for energy use forecast in non-residential buildings. *Scientific Reports*, *12*(1), 1065.
Pathak, V. K., & Srivastava, A. K. (2022). A novel upgraded bat algorithm based on cuckoo search and Sugeno inertia weight for large scale and constrained engineering design optimization problems. *Engineering with computers*, *38*(2), 1731-1758.
Peng, L., Cai, Z., Heidari, A. A., Zhang, L., & Chen, H. (2023). Hierarchical Harris hawks optimizer for feature selection. *Journal of Advanced Research*.
Qian, Y., Tu, J., Luo, G., Sha, C., Heidari, A. A., & Chen, H. (2023). Multi-threshold remote sensing image segmentation with improved ant colony optimizer with salp foraging. *Journal of Computational Design and Engineering*, *10*(6), 2200-2221.
Qiao, L., Liu, K., Xue, Y., Tang, W., & Salehnia, T. (2024). A multi-level thresholding image segmentation method using hybrid Arithmetic Optimization and Harris Hawks Optimizer algorithms. *Expert Systems with Applications*, *241*, 122316.
Rajwar, K., Deep, K., & Das, S. (2023). An exhaustive review of the metaheuristic algorithms for search and optimization: taxonomy, applications, and open challenges. *Artificial Intelligence Review*, 1-71.
Rao, R. V., Savsani, V. J., & Vakharia, D. (2011). Teaching–learning-based optimization: a novel method for constrained mechanical design optimization problems. *Computer-aided design*, *43*(3), 303-315.
Rashedi, E., Nezamabadi-Pour, H., & Saryazdi, S. (2009). GSA: a gravitational search algorithm. *Information Sciences*, *179*(13), 2232-2248.
Reski, R. (1998). Development, genetics and molecular biology of mosses. *Botanica Acta*, *111*(1), 1-15.
Richards, D., & Amos, M. (2016). Shape optimization with surface-mapped CPPNs. *IEEE Transactions on Evolutionary Computation*, *21*(3), 391-407.
Rosenstiel, T. N., Shortlidge, E. E., Melnychenko, A. N., Pankow, J. F., & Eppley, S. M. (2012). Sex-specific volatile compounds influence microarthropod-mediated fertilization of moss. *Nature*, *489*(7416), 431-433.
Sahoo, S. K., Houssein, E. H., Premkumar, M., Saha, A. K., & Emam, M. M. (2023). Self-adaptive moth flame optimizer combined with crossover operator and Fibonacci search strategy for COVID-19 CT image segmentation. *Expert Systems with Applications*, *227*, 120367.
Schaefer, D. G., & Zrÿd, J.-P. (2001). The moss Physcomitrella patens, now and then. *Plant physiology*, *127*(4), 1430-1438.
Sheskin, D. J. (2003). *Handbook of parametric and nonparametric statistical procedures*. Chapman and hall/CRC.

Simon, D. (2008). Biogeography-based optimization. *IEEE Transactions on Evolutionary Computation*, *12*(6), 702-713.
Storn, R., & Price, K. (1997). Differential evolution–a simple and efficient heuristic for global optimization over continuous spaces. *Journal of Global Optimization*, *11*, 341-359.
Su, H., Zhao, D., Heidari, A. A., Liu, L., Zhang, X., Mafarja, M., & Chen, H. (2023). RIME: A physics-based optimization. *Neurocomputing*, *532*, 183-214. https://doi.org/10.1016/j.neucom.2023.02.010
Sun, G., Xu, Z., Yu, H., Chen, X., Chang, V., & Vasilakos, A. V. (2019). Low-latency and resource-efficient service function chaining orchestration in network function virtualization. *IEEE Internet of Things Journal*, *7*(7), 5760-5772.
Sun, G., Zhang, Y., Liao, D., Yu, H., Du, X., & Guizani, M. (2018). Bus-trajectory-based street-centric routing for message delivery in urban vehicular ad hoc networks. *IEEE Transactions on Vehicular Technology*, *67*(8), 7550-7563.
Tubishat, M., Abushariah, M. A., Idris, N., & Aljarah, I. (2019). Improved whale optimization algorithm for feature selection in Arabic sentiment analysis. *Applied Intelligence*, *49*, 1688-1707.
Villalón, C. L. C., Stützle, T., & Dorigo, M. (2020). Grey Wolf, Firefly and Bat Algorithms: Three Widespread Algorithms that Do Not Contain Any Novelty. International Conference on Swarm Intelligence,
Wang, C., Wang, Y., Wang, K., Dong, Y., & Yang, Y. (2017). An Improved Hybrid Algorithm Based on Biogeography/Complex and Metropolis for Many-Objective Optimization. *Mathematical Problems in Engineering*, *2017*, 2462891. https://doi.org/10.1155/2017/2462891
Wang, P., Xue, B., Liang, J., & Zhang, M. (2022). Differential evolution with duplication analysis for feature selection in classification. *IEEE Transactions on Cybernetics*.
Wang, R., & Zhang, R. (2023). Techno-economic analysis and optimization of hybrid energy systems based on hydrogen storage for sustainable energy utilization by a biological-inspired optimization algorithm. *Journal of Energy Storage*, *66*, 107469.
Wang, S., Jia, H., Hussien, A. G., Abualigah, L., Lin, G., Wei, H., Lin, Z., & Dhal, K. G. (2024). Boosting aquila optimizer by marine predators algorithm for combinatorial optimization. *Journal of Computational Design and Engineering*, *11*(2), 37-69.
Wolpert, D. H., & Macready, W. G. (1997). No free lunch theorems for optimization. *IEEE Transactions on Evolutionary Computation*, *1*(1), 67-82.
Wu, G., Mallipeddi, R., & Suganthan, P. N. (2017). Problem definitions and evaluation criteria for the CEC 2017 competition on constrained real-parameter optimization. *National University of Defense Technology, Changsha, Hunan, PR China and Kyungpook National University, Daegu, South Korea and Nanyang Technological University, Singapore, Technical Report*.
Xia, X., Gui, L., & Zhan, Z.-H. (2018). A multi-swarm particle swarm optimization algorithm based on dynamical topology and purposeful detecting. *Applied Soft Computing*, *67*, 126-140. https://doi.org/10.1016/j.asoc.2018.02.042
Xie, L., Zeng, J., & Cui, Z. (2009). General framework of artificial physics optimization algorithm. 2009 world congress on nature & biologically inspired computing (NaBIC),

Xie, X., Xia, F., Wu, Y., Liu, S., Yan, K., Xu, H., & Ji, Z. (2023). A Novel Feature Selection Strategy Based on Salp Swarm Algorithm for Plant Disease Detection. *Plant Phenomics*, *5*, 0039.

Xu, X., & Wei, Z. (2023). Dynamic pickup and delivery problem with transshipments and LIFO constraints. *Computers & Industrial Engineering*, *175*, 108835.

Yang, X.-S. (2009). Firefly algorithms for multimodal optimization. International symposium on stochastic algorithms,

Yang, X.-S. (2010). A new metaheuristic bat-inspired algorithm. In *Nature inspired cooperative strategies for optimization (NICSO 2010)* (pp. 65-74). Springer.

Yang, X. S., & Hossein Gandomi, A. (2012). Bat algorithm: a novel approach for global engineering optimization. *Engineering computations*, *29*(5), 464-483.

Yao, X., Liu, Y., & Lin, G. (1999). Evolutionary programming made faster. *IEEE Transactions on Evolutionary Computation*, *3*(2), 82-102.

Yin, L., Zhuang, M., Jia, J., & Wang, H. (2020). Energy saving in flow-shop scheduling management: an improved multiobjective model based on grey wolf optimization algorithm. *Mathematical Problems in Engineering*, *2020*, 1-14.

Zhang, J., Wei, L., Guo, Z., Sun, H., & Hu, Z. (2024). A survey of meta-heuristic algorithms in optimization of space scale expansion. *Swarm and Evolutionary Computation*, *84*, 101462.

Zhao, W., Wang, L., & Zhang, Z. (2019). Atom search optimization and its application to solve a hydrogeologic parameter estimation problem. *Knowledge-Based Systems*, *163*, 283-304.

Zhao, W., Wang, L., Zhang, Z., Fan, H., Zhang, J., Mirjalili, S., Khodadadi, N., & Cao, Q. (2024). Electric eel foraging optimization: A new bio-inspired optimizer for engineering applications. *Expert Systems with Applications*, *238*, 122200.

Zhao, W., Wang, L., Zhang, Z., Mirjalili, S., Khodadadi, N., & Ge, Q. (2023). Quadratic Interpolation Optimization (QIO): A new optimization algorithm based on generalized quadratic interpolation and its applications to real-world engineering problems. *Computer Methods in Applied Mechanics and Engineering*, *417*, 116446.

Appendix

A. Specific mean and variance statistics

This section presents the average and variance of the optimal results obtained from 30 independent experiments. The bolded text indicates the algorithms that attained the optimal mean or variance in the test functions. Table A1 shows the comparison results of MGO in CEC 2017 with original algorithms, Table A2 shows the comparison results of MGO in CEC 2017 with advanced algorithms, Table A3 shows the comparison results of MGO in CEC 2022 with other algorithms, and Table A4 shows the experimental results of MGO in CEC 2017 for different dimensions.

Table A1. Results of MGO and original algorithms on CEC 2017.

	F1		F3		F4	
	Avg	Std	Avg	Std	Avg	Std
MG	2.8990E+05	7.5260E+05	5.2823E+03	1.7689E+03	4.8922E+02	**8.8258E+00**
SM	2.6600E+06	7.2249E+06	4.9535E+03	2.5939E+03	5.0137E+02	2.4575E+01
RIM	**8.0964E+03**	**6.8071E+03**	3.0172E+02	7.3648E-01	4.8667E+02	2.3446E+01
HH	1.1253E+07	2.6981E+06	7.9118E+03	2.8003E+03	5.2500E+02	2.1489E+01
WO	2.3166E+06	1.5860E+06	1.7219E+05	6.1037E+04	5.4646E+02	4.2559E+01
PSO	1.3961E+08	1.1263E+07	6.5478E+02	5.8008E+01	4.8691E+02	3.0062E+01
SCA	1.2880E+10	1.6715E+09	3.6018E+04	6.6031E+03	1.4060E+03	2.1763E+02
MF	1.2355E+10	7.3768E+09	1.1304E+05	7.8423E+04	1.2915E+03	7.8544E+02
FA	1.4659E+10	1.5813E+09	5.8853E+04	9.9906E+03	1.3570E+03	1.5809E+02
GW	1.5837E+09	1.0828E+09	3.5069E+04	1.2256E+04	5.8493E+02	7.9335E+01
BA	5.2578E+05	2.9092E+05	**3.0012E+02**	**1.1078E-01**	**4.7943E+02**	2.4400E+01
	F5		F6		F7	
	Avg	Std	Avg	Std	Avg	Std
MG	**5.5322E+02**	**9.3729E+00**	**6.0000E+02**	**4.2859E-05**	**7.8392E+02**	**9.7234E+00**
SM	6.2329E+02	2.7058E+01	6.1544E+02	5.6769E+00	9.2865E+02	5.9732E+01
RIM	5.8313E+02	2.4475E+01	6.0037E+02	2.5259E-01	8.1132E+02	2.2337E+01
HH	7.3084E+02	3.1085E+01	6.6147E+02	6.0380E+00	1.2621E+03	6.7830E+01
WO	7.9836E+02	5.9206E+01	6.7146E+02	8.4988E+00	1.2760E+03	1.0831E+02
PSO	7.4564E+02	3.3985E+01	6.4889E+02	1.2030E+01	9.1821E+02	1.9607E+01
SCA	7.7528E+02	1.5085E+01	6.4844E+02	4.4876E+00	1.1292E+03	3.0505E+01
MF	7.2648E+02	5.5566E+01	6.4161E+02	1.0668E+01	1.1994E+03	2.1677E+02
FA	7.6155E+02	1.1957E+01	6.4350E+02	2.3742E+00	1.3760E+03	4.6864E+01
GW	5.9605E+02	2.1795E+01	6.0765E+02	2.8467E+00	8.6212E+02	4.4477E+01
BA	8.3648E+02	7.1984E+01	6.7000E+02	1.0573E+01	1.6262E+03	2.2182E+02
	F8		F9		F10	
	Avg	Std	Avg	Std	Avg	Std
MG	**8.5340E+02**	**8.8935E+00**	**9.0464E+02**	**7.3657E+00**	**3.6460E+03**	3.4879E+02
SM	9.1685E+02	2.5619E+01	3.3039E+03	8.6718E+02	4.1082E+03	6.3715E+02
RIM	8.8389E+02	1.7287E+01	1.3497E+03	4.5617E+02	3.6710E+03	6.5228E+02
HH	9.5994E+02	2.8725E+01	6.7258E+03	7.1443E+02	5.6201E+03	7.7764E+02
WO	1.0215E+03	5.6691E+01	7.0498E+03	1.8190E+03	6.2773E+03	9.2699E+02
PSO	9.8613E+02	2.3285E+01	5.3125E+03	1.8324E+03	5.9884E+03	5.2418E+02
SCA	1.0452E+03	1.8791E+01	5.2081E+03	9.5675E+02	8.1644E+03	**3.1937E+02**
MF	1.0262E+03	4.8916E+01	7.5704E+03	2.3656E+03	5.4475E+03	8.3125E+02
FA	1.0517E+03	1.2697E+01	5.4286E+03	4.4764E+02	7.9533E+03	3.2627E+02
GW	8.9105E+02	1.5796E+01	1.8810E+03	5.2023E+02	3.9441E+03	4.0899E+02
BA	1.0441E+03	4.0385E+01	1.4416E+04	5.6551E+03	5.7002E+03	7.0442E+02
	F11		F12		F13	
	Avg	Std	Avg	Std	Avg	Std
MG	**1.1791E+03**	**2.2601E+01**	**5.9778E+05**	**4.6525E+05**	2.3541E+04	1.8362E+04

SM	1.2257E+03	2.8112E+01	3.1666E+06	2.2854E+06	4.3077E+04	2.8343E+04
RIM	1.1880E+03	3.8611E+01	2.2466E+06	1.9825E+06	**1.4218E+04**	**1.3208E+04**
HH	1.2400E+03	3.7815E+01	1.1232E+07	7.4248E+06	3.2443E+05	2.0001E+05
WO	1.5260E+03	2.4129E+02	5.0574E+07	3.5734E+07	1.5149E+05	1.0280E+05
PSO	1.2896E+03	4.5147E+01	2.6097E+07	1.1845E+07	4.5392E+06	1.0214E+06
SCA	2.1166E+03	2.6616E+02	1.1842E+09	2.9578E+08	3.9758E+08	1.2891E+08
MF	5.2127E+03	7.4794E+03	3.2619E+08	4.7086E+08	6.1105E+06	1.7942E+07
FA	3.4558E+03	5.3914E+02	1.5424E+09	2.7408E+08	6.4351E+08	1.5545E+08
GW	2.0315E+03	6.9291E+02	4.4746E+07	5.2929E+07	1.5896E+06	5.7885E+06
BA	1.3113E+03	7.1005E+01	2.6687E+06	2.0698E+06	2.7702E+05	1.0153E+05
	F14		F15		F16	
	Avg	Std	Avg	Std	Avg	Std
MG	7.8529E+03	**4.3426E+03**	**1.0845E+04**	**6.4665E+03**	**2.1474E+03**	**1.5707E+02**
SM	4.8347E+04	3.1652E+04	2.1345E+04	1.3239E+04	2.5747E+03	2.7469E+02
RIM	1.7271E+04	9.4420E+03	1.3100E+04	1.2306E+04	2.3420E+03	2.4336E+02
HH	4.0496E+04	2.7321E+04	6.2499E+04	3.9194E+04	3.1945E+03	3.8470E+02
WO	6.9560E+05	7.5884E+05	7.3718E+04	6.1664E+04	3.5920E+03	4.4798E+02
PSO	1.1117E+04	7.1797E+03	4.5936E+05	1.7647E+05	2.8854E+03	2.1979E+02
SCA	1.4935E+05	5.3731E+04	1.1466E+07	9.3152E+06	3.5622E+03	2.6880E+02
MF	5.0650E+05	1.9155E+06	6.9322E+04	7.8189E+04	3.1383E+03	4.1902E+02
FA	1.9779E+05	8.4694E+04	6.3280E+07	2.7958E+07	3.4383E+03	1.6047E+02
GW	1.8713E+05	3.0241E+05	1.7696E+05	4.6491E+05	2.3693E+03	2.8952E+02
BA	**6.2210E+03**	4.3864E+03	1.0923E+05	5.7837E+04	3.3992E+03	4.3953E+02
	F17		F18		F19	
	Avg	Std	Avg	Std	Avg	Std
MG	**1.8590E+03**	**4.5645E+01**	2.1311E+05	**1.0250E+05**	**7.4845E+03**	**6.0406E+03**
SM	2.2327E+03	2.0149E+02	3.7079E+05	2.8613E+05	1.5381E+04	1.9386E+04
RIM	2.0297E+03	1.4133E+02	2.9547E+05	2.5060E+05	1.2911E+04	1.2343E+04
HH	2.6559E+03	2.7858E+02	1.1273E+06	1.3388E+06	2.9592E+05	1.7420E+05
WO	2.5756E+03	2.3442E+02	2.1831E+06	2.1590E+06	3.3446E+06	2.7047E+06
PSO	2.4060E+03	2.5920E+02	2.5222E+05	1.9834E+05	1.2759E+06	6.6934E+05
SCA	2.4155E+03	1.5535E+02	3.3299E+06	1.8080E+06	2.5407E+07	1.0597E+07
MF	2.5554E+03	2.4468E+02	2.3546E+06	4.6962E+06	1.0574E+07	3.4948E+07
FA	2.4928E+03	1.3178E+02	3.9747E+06	1.4000E+06	9.6433E+07	3.6296E+07
GW	2.0111E+03	1.6523E+02	7.0065E+05	1.3102E+06	7.3938E+05	9.8454E+05
BA	2.8331E+03	2.4093E+02	**1.8476E+05**	1.2947E+05	6.3662E+05	2.4511E+05
	F20		F21		F22	
	Avg	Std	Avg	Std	Avg	Std
MG	**2.1994E+03**	**7.7190E+01**	**2.3517E+03**	2.0164E+01	**2.7079E+03**	1.0437E+03
SM	2.4529E+03	1.5484E+02	2.3992E+03	2.2017E+01	5.1280E+03	1.4419E+03
RIM	2.3357E+03	1.3383E+02	2.3885E+03	1.6829E+01	3.8968E+03	1.4652E+03
HH	2.7569E+03	2.4584E+02	2.5397E+03	6.0469E+01	5.9307E+03	2.2888E+03
WO	2.8070E+03	2.1071E+02	2.5762E+03	6.7688E+01	6.6701E+03	2.2481E+03

PSO	2.6233E+03	1.6346E+02	2.5315E+03	3.7721E+01	5.4086E+03	2.6065E+03
SCA	2.5961E+03	1.0677E+02	2.5545E+03	2.0603E+01	8.6493E+03	2.0453E+03
MF	2.6607E+03	2.1741E+02	2.5007E+03	5.2908E+01	6.3048E+03	1.6583E+03
FA	2.5975E+03	1.0616E+02	2.5389E+03	**1.3834E+01**	3.8636E+03	**1.2139E+02**
GW	2.3667E+03	1.2278E+02	2.3882E+03	2.4171E+01	4.3301E+03	1.7810E+03
BA	2.9528E+03	2.1027E+02	2.6140E+03	5.9534E+01	7.1598E+03	6.0840E+02
	F23		F24		F25	
	Avg	Std	Avg	Std	Avg	Std
MG	**2.7091E+03**	**1.5257E+01**	**2.8748E+03**	4.9898E+01	**2.8871E+03**	**4.6854E-01**
SM	2.7717E+03	2.2816E+01	2.9611E+03	3.4644E+01	2.8992E+03	2.4279E+01
RIM	2.7380E+03	2.2366E+01	2.9240E+03	3.2009E+01	2.8916E+03	1.2458E+01
HH	3.1533E+03	1.2458E+02	3.3905E+03	1.5139E+02	2.9144E+03	2.0591E+01
WO	3.0365E+03	7.8008E+01	3.1434E+03	8.9070E+01	2.9496E+03	3.7525E+01
PSO	3.1054E+03	1.2348E+02	3.2216E+03	1.2736E+02	2.9108E+03	2.9827E+01
SCA	2.9844E+03	3.1407E+01	3.1610E+03	2.3728E+01	3.1900E+03	5.8766E+01
MF	2.8354E+03	3.7331E+01	2.9906E+03	3.2899E+01	3.2710E+03	4.0773E+02
FA	2.9115E+03	1.5604E+01	3.0641E+03	**1.3547E+01**	3.5882E+03	1.0849E+02
GW	2.7553E+03	3.1757E+01	2.9233E+03	5.0046E+01	2.9831E+03	3.5482E+01
BA	3.3307E+03	1.5814E+02	3.3431E+03	1.1880E+02	2.9112E+03	2.3209E+01
	F26		F27		F28	
	Avg	Std	Avg	Std	Avg	Std
MG	**4.0186E+03**	3.9639E+02	3.2083E+03	**4.4499E+00**	3.2194E+03	**1.2742E+01**
SM	4.8778E+03	2.2243E+02	3.2255E+03	1.7849E+01	3.2407E+03	2.6577E+01
RIM	4.4857E+03	5.8662E+02	3.2198E+03	1.1417E+01	3.2184E+03	2.1823E+01
HH	6.7470E+03	1.3522E+03	3.3562E+03	1.0669E+02	3.2524E+03	2.2836E+01
WO	7.8913E+03	8.7146E+02	3.3950E+03	1.0721E+02	3.3013E+03	4.1557E+01
PSO	4.6470E+03	1.9225E+03	**3.1653E+03**	3.8830E+01	3.2432E+03	2.1243E+01
SCA	7.0302E+03	3.0005E+02	3.3962E+03	3.7136E+01	3.7846E+03	1.0940E+02
MF	5.7867E+03	5.1565E+02	3.2518E+03	3.5325E+01	4.3510E+03	8.6598E+02
FA	6.5408E+03	**1.7887E+02**	3.3334E+03	1.7574E+01	3.9254E+03	9.5191E+01
GW	4.6037E+03	4.8841E+02	3.2579E+03	3.2886E+01	3.3967E+03	8.0863E+01
BA	8.9385E+03	2.4335E+03	3.4211E+03	1.2336E+02	**3.1185E+03**	4.3142E+01
	F29		F30			
	Avg	Std	Avg	Std		
MG	**3.5823E+03**	**9.2845E+01**	4.7078E+04	3.9615E+04		
SM	3.8440E+03	2.0144E+02	2.6378E+04	**1.3271E+04**		
RIM	3.5922E+03	1.4086E+02	**2.6142E+04**	3.0790E+04		
HH	4.3275E+03	2.7912E+02	1.8603E+06	1.0920E+06		
WO	4.8366E+03	4.7333E+02	1.0888E+07	7.6156E+06		
PSO	4.3005E+03	2.8285E+02	3.2591E+06	1.4546E+06		
SCA	4.7235E+03	2.0852E+02	7.3614E+07	2.9620E+07		
MF	4.1477E+03	2.3358E+02	7.2809E+05	9.3522E+05		
FA	4.6628E+03	1.4080E+02	9.7760E+07	2.6026E+07		

GW	3.7070E+03	1.5395E+02	7.4817E+06	6.4047E+06
BA	4.9707E+03	3.7763E+02	1.4239E+06	8.4549E+05

Table A2. Results of MGO and advanced algorithms on CEC 2017.

	F1		F3		F4	
	Avg	Std	Avg	Std	Avg	Std
MGO	1.7106E+	2.3484E+	5.8220E+	2.1318E+	4.8913E+	1.2907E+0
SCAD	1.9417E+	3.1871E+	6.1225E+	6.5015E+	3.6278E+	8.4935E+0
IWO	2.4734E+	2.5179E+	8.0673E+	3.2523E+	5.3351E+	3.1783E+0
RCBA	1.7118E+	5.3907E+	3.0105E+	3.2819E-	4.8524E+	2.6184E+0
OBSC	1.7366E+	2.5837E+	6.1086E+	8.0911E+	2.6355E+	7.1634E+0
ALCP	6.4670E+	6.6662E+	2.7024E+	3.9714E+	5.0786E+	4.7290E+0
CMA	**1.0000E+**	**3.7320E-**	**3.0000E+**	**2.5856E-**	4.3540E+	2.8864E+0
OBL	1.5145E+	9.7533E+	1.9250E+	5.1944E+	5.2136E+	2.8758E+0
CGSC	1.4933E+	2.6057E+	4.4082E+	6.7183E+	1.7260E+	3.3523E+0
RDW	1.4824E+	3.4433E+	2.2018E+	8.2190E+	5.0879E+	2.8029E+0
MSPS	1.1582E+	6.6989E+	3.0000E+	2.0475E-	**4.0292E+**	**1.7931E+0**

	F5		F6		F7	
	Avg	Std	Avg	Std	Avg	Std
MGO	**5.5254E+**	**9.4478E+**	**6.0000E+**	**9.5452E-**	**7.8063E+**	**1.0012E+0**
SCAD	8.3004E+	2.2864E+	6.5978E+	7.2550E+	1.1783E+	4.8469E+0
IWO	7.5893E+	6.2020E+	6.5338E+	1.1137E+	1.1748E+	9.0955E+0
RCBA	8.0691E+	4.7188E+	6.7141E+	9.4720E+	1.9026E+	2.7699E+0
OBSC	8.0925E+	2.1952E+	6.5563E+	5.3935E+	1.1829E+	4.4224E+0
ALCP	5.9544E+	3.0970E+	6.0541E+	5.4423E+	8.6266E+	4.1973E+0
CMA	1.2355E+	1.9202E+	6.9026E+	1.4946E+	4.1289E+	1.0639E+0
OBL	6.6289E+	3.8639E+	6.2134E+	1.5021E+	9.2675E+	6.5454E+0
CGSC	7.9926E+	1.6250E+	6.5596E+	5.8246E+	1.1351E+	3.3663E+0
RDW	6.8304E+	4.9500E+	6.1645E+	7.5291E+	9.9334E+	6.5064E+0
MSPS	6.8576E+	2.5954E+	6.4785E+	4.5910E+	8.0370E+	1.9144E+0

	F8		F9		F10	
	Avg	Std	Avg	Std	Avg	Std
MGO	**8.5129E+**	**1.1576E+**	**9.0624E+**	**8.8247E+**	**3.8488E+**	3.3485E+0
SCAD	1.0823E+	1.5621E+	8.3868E+	1.0794E+	8.1190E+	3.4717E+0
IWO	9.9250E+	4.1941E+	7.0181E+	2.2231E+	5.5787E+	6.1739E+0
RCBA	1.0727E+	5.2326E+	8.7635E+	2.7117E+	5.5534E+	6.9607E+0
OBSC	1.0678E+	2.2547E+	6.6972E+	1.0979E+	7.2597E+	4.4485E+0
ALCP	9.0661E+	2.8816E+	2.0219E+	1.2873E+	4.3521E+	4.3322E+0
CMA	1.3643E+	1.1764E+	1.4513E+	3.3668E+	6.1856E+	7.8108E+0
OBL	9.4610E+	3.9623E+	3.4860E+	1.7449E+	5.2240E+	8.1048E+0
CGSC	1.0574E+	1.6749E+	6.1580E+	1.1106E+	8.1840E+	**2.4573E+**
RDW	9.8284E+	3.9627E+	4.6471E+	1.4273E+	4.7837E+	7.3125E+0
MSPS	9.3200E+	2.2729E+	3.6696E+	9.2561E+	4.4140E+	3.6122E+0

	F11		F12		F13	
	Avg	Std	Avg	Std	Avg	Std
MGO	**1.1840E+**	2.6654E+	6.2205E+	4.2170E+	2.4553E+	1.4584E+0
SCAD	3.4226E+	6.7446E+	1.9724E+	4.9635E+	6.5829E+	2.1154E+0
IWO	1.3522E+	6.2408E+	1.0620E+	7.9669E+	3.4165E+	2.5889E+0
RCBA	1.3032E+	6.0382E+	1.5159E+	9.1061E+	1.1612E+	6.6144E+0
OBSC	2.9398E+	7.0487E+	2.0194E+	4.3574E+	6.7670E+	3.6109E+0
ALCP	1.2597E+	6.3084E+	3.6267E+	4.9679E+	2.6006E+	2.3099E+0
CMA	1.3036E+	7.1416E+	2.6841E+	4.3861E+	2.9734E+	**5.9458E+**
OBL	1.2879E+	4.3212E+	1.6848E+	1.2247E+	1.9625E+	1.3831E+0
CGSC	2.1993E+	2.3950E+	1.3847E+	3.1748E+	4.7011E+	1.8238E+0
RDW	1.2338E+	5.6172E+	3.3983E+	2.0509E+	1.4870E+	1.8596E+0
MSPS	1.1901E+	**2.3918E+**	**2.6445E+**	**5.2133E+**	**2.8894E+**	8.5094E+0
	F14		F15		F16	
	Avg	Std	Avg	Std	Avg	Std
MGO	7.9868E+	4.5004E+	1.2338E+	1.1276E+	**2.1586E+**	**1.1486E+0**
SCAD	3.6470E+	1.7976E+	9.4117E+	5.9941E+	3.8844E+	2.2834E+0
IWO	3.3656E+	3.8458E+	1.7120E+	1.0038E+	3.1255E+	3.3766E+0
RCBA	8.0764E+	3.9362E+	4.4948E+	3.6158E+	3.2112E+	5.6083E+0
OBSC	3.0309E+	1.3298E+	1.1463E+	1.3831E+	3.8111E+	1.6560E+0
ALCP	2.7653E+	4.6398E+	1.2628E+	1.1912E+	2.5147E+	3.2234E+0
CMA	1.6037E+	6.5564E+	**1.7724E+**	1.3295E+	2.1924E+	3.6919E+0
OBL	5.0953E+	4.4432E+	9.1594E+	5.2043E+	2.8603E+	4.2953E+0
CGSC	1.9065E+	2.6040E+	1.1527E+	1.2527E+	3.7155E+	1.9115E+0
RDW	1.5526E+	1.4657E+	1.0946E+	1.1754E+	2.7796E+	3.6440E+0
MSPS	**1.5730E+**	**8.9908E+**	1.8083E+	**9.2613E+**	2.5940E+	3.0857E+0
	F17		F18		F19	
	Avg	Std	Avg	Std	Avg	Std
MGO	**1.8365E+**	**3.6755E+**	1.7766E+	8.2603E+	7.9786E+	6.9311E+0
SCAD	2.5329E+	1.6460E+	4.1177E+	2.0420E+	3.1949E+	2.4783E+0
IWO	2.4108E+	2.2596E+	1.7904E+	1.8699E+	1.7557E+	2.4970E+0
RCBA	2.8553E+	4.0410E+	1.8434E+	1.1857E+	1.3084E+	1.2208E+0
OBSC	2.5431E+	1.8613E+	4.8958E+	3.0485E+	4.2617E+	2.0854E+0
ALCP	2.1924E+	1.8862E+	1.8028E+	1.6394E+	1.5102E+	1.5432E+0
CMA	2.0204E+	1.6853E+	**2.0208E+**	8.8971E+	**2.0966E+**	**7.7248E+**
OBL	2.2141E+	2.0943E+	1.3006E+	1.0039E+	4.2477E+	3.2826E+0
CGSC	2.4817E+	1.8232E+	3.0036E+	1.7743E+	2.9465E+	2.0634E+0
RDW	2.1954E+	2.6042E+	4.5943E+	4.5788E+	1.3431E+	1.3912E+0
MSPS	2.1381E+	2.0656E+	2.0291E+	**5.1671E+**	2.2049E+	2.2528E+0
	F20		F21		F22	
	Avg	Std	Avg	Std	Avg	Std
MGO	**2.1878E+**	**7.0304E+**	**2.3510E+**	**1.7428E+**	2.9754E+	1.2421E+0
SCAD	2.7117E+	8.5457E+	2.5791E+	2.0282E+	4.5183E+	3.9522E+0

IWO	2.6158E+	1.7459E+	2.5511E+	4.7953E+	6.0931E+	2.2350E+0
RCBA	2.9697E+	2.5984E+	2.6274E+	7.4871E+	7.3786E+	7.9617E+0
OBSC	2.6624E+	1.2203E+	2.4670E+	7.5167E+	4.1796E+	3.6642E+0
ALCP	2.3851E+	1.7252E+	2.4153E+	3.4920E+	4.4460E+	1.8484E+0
CMA	3.4017E+	3.1232E+	2.5875E+	2.7327E+	7.9974E+	1.1730E+0
OBL	2.5275E+	1.4114E+	2.4387E+	3.8564E+	**2.8061E+**	1.4884E+0
CGSC	2.6321E+	1.1163E+	2.5692E+	1.9707E+	3.8642E+	**2.3199E+0**
RDW	2.4626E+	1.8438E+	2.4932E+	4.7327E+	6.3308E+	1.2743E+0
MSPS	2.4470E+	1.0290E+	2.4352E+	2.3817E+	3.0183E+	1.6398E+0

	F23		F24		F25	
	Avg	Std	Avg	Std	Avg	Std
MGO	**2.7114E+**	**1.5635E+**	2.8817E+	**1.3158E+**	**2.8869E+**	**8.8596E-**
SCAD	3.0061E+	3.2310E+	3.1704E+	3.0100E+	3.4892E+	9.2620E+0
IWO	2.9665E+	8.5186E+	3.1658E+	8.6104E+	2.9437E+	3.3132E+0
RCBA	3.3875E+	2.0852E+	3.4051E+	1.8364E+	2.8968E+	2.2118E+0
OBSC	3.0170E+	2.8328E+	3.1888E+	3.5749E+	3.3977E+	1.2726E+0
ALCP	2.7838E+	4.7144E+	2.9730E+	5.5778E+	2.8975E+	2.1793E+0
CMA	4.3759E+	8.2095E+	**2.8712E+**	4.6397E+	2.8880E+	3.4573E+0
OBL	2.7981E+	3.5862E+	2.9792E+	4.0213E+	2.9114E+	2.4559E+0
CGSC	2.9930E+	3.1271E+	3.1468E+	2.8012E+	3.3069E+	1.0619E+0
RDW	2.8551E+	4.8003E+	3.1512E+	1.1050E+	2.9072E+	1.9920E+0
MSPS	2.9837E+	1.2728E+	3.0753E+	6.4987E+	2.8971E+	2.2151E+0

	F26		F27		F28	
	Avg	Std	Avg	Std	Avg	Std
MGO	3.9874E+	**3.4702E+**	**3.2087E+**	**5.0094E+**	3.2232E+	**1.0957E+0**
SCAD	7.3969E+	3.6436E+	3.4491E+	5.4004E+	4.2213E+	2.2396E+0
IWO	6.8634E+	1.0195E+	3.3172E+	5.9386E+	3.2914E+	3.0958E+0
RCBA	9.0680E+	2.1248E+	3.4816E+	1.9404E+	3.1869E+	5.6702E+0
OBSC	6.9704E+	6.7402E+	3.4477E+	5.7765E+	4.2068E+	2.4474E+0
ALCP	4.9239E+	9.8615E+	3.2461E+	2.2529E+	3.2493E+	6.2133E+0
CMA	**3.6353E+**	4.9953E+	3.4131E+	1.2248E+	3.1389E+	5.7043E+0
OBL	5.1056E+	9.8225E+	3.2390E+	1.5859E+	3.2791E+	3.6164E+0
CGSC	7.0292E+	5.1319E+	3.3870E+	3.6426E+	3.9596E+	1.3021E+0
RDW	5.8780E+	1.1151E+	3.2510E+	2.3054E+	3.2593E+	2.3796E+0
MSPS	5.0340E+	2.0972E+	3.2845E+	8.1211E+	**3.1227E+**	4.6891E+0

	F29		F30	
	Avg	Std	Avg	Std
MGO	**3.5987E+**	**6.4548E+**	4.3473E+	2.7873E+
SCAD	5.1117E+	2.2695E+	1.0761E+	3.7638E+
IWO	4.2311E+	2.5591E+	6.4172E+	4.8268E+
RCBA	4.8766E+	4.3385E+	2.2596E+	1.5570E+
OBSC	4.9029E+	2.9509E+	1.1638E+	4.2666E+
ALCP	3.8511E+	2.3928E+	1.7376E+	1.4165E+

CMA	3.6850E+	1.6374E+	**5.1775E+**	**1.5641E+**
OBL	3.9906E+	2.3812E+	2.7935E+	1.8521E+
CGSC	4.7703E+	2.3970E+	9.3986E+	3.9529E+
RDW	3.9685E+	1.9626E+	1.7563E+	8.8609E+
MSPS	4.0192E+	2.3166E+	9.3043E+	2.1261E+

Table A3. Results of MGO and other algorithms in CEC 2022.

	F1		F2		F3	
	Avg	Std	Avg	Std	Avg	Std
MGO	3.0409E+02	4.4871E+00	4.4126E+02	1.1594E+01	**6.0000E+02**	**2.0260E-06**
MSPS	**3.0000E+02**	**1.2779E-08**	**4.0013E+02**	**7.2785E-01**	6.4214E+02	7.0299E+00
ALCP	4.3155E+03	1.2803E+03	4.5252E+02	2.0977E+01	6.0078E+02	2.3545E+00
IWO	8.0300E+02	8.7723E+02	4.5379E+02	1.5768E+01	6.3932E+02	1.0564E+01
SCAD	2.1520E+04	3.4086E+03	7.4399E+02	7.5190E+01	6.4049E+02	6.2945E+00
OBL	4.2393E+02	5.7119E+01	4.5992E+02	1.2228E+01	6.0752E+02	8.4489E+00
RIME	3.0001E+02	6.5296E-03	4.4596E+02	1.5745E+01	6.0005E+02	3.2205E-02
GWO	8.1807E+03	4.2591E+03	4.9251E+02	3.4285E+01	6.0335E+02	2.7708E+00
PSO	3.7426E+02	9.8310E+00	4.3555E+02	2.5972E+01	6.3588E+02	1.3622E+01
WOA	1.2844E+03	9.4266E+02	4.7470E+02	2.5355E+01	6.5853E+02	1.6438E+01
SCA	7.6912E+03	2.3573E+03	6.2372E+02	4.4716E+01	6.3397E+02	3.5708E+00
	F4		F5		F6	
	Avg	Std	Avg	Std	Avg	Std
MGO	**8.2993E+02**	**5.4490E+00**	**9.0147E+02**	**2.5665E+00**	6.8151E+03	6.3215E+03
MSPS	8.6812E+02	1.1632E+01	1.5476E+03	3.8340E+02	**1.8838E+03**	**2.0336E+01**
ALCP	8.6557E+02	2.0895E+01	1.0854E+03	2.0520E+02	7.8625E+03	6.0922E+03
IWO	9.0831E+02	3.4011E+01	3.3347E+03	1.0575E+03	8.6898E+03	7.1792E+03
SCAD	9.4714E+02	7.9987E+00	2.4125E+03	3.5709E+02	6.3191E+07	4.8142E+07
OBL	8.7223E+02	2.0548E+01	1.2160E+03	5.0237E+02	2.3391E+04	2.4240E+04
RIME	8.5028E+02	1.4302E+01	9.1125E+02	2.3709E+01	6.2694E+03	5.1695E+03
GWO	8.4403E+02	1.6043E+01	1.1103E+03	1.7108E+02	6.1992E+05	2.3606E+06
PSO	8.8722E+02	1.8943E+01	1.2533E+03	6.2697E+02	1.2071E+06	4.1383E+05
WOA	9.1173E+02	3.2021E+01	3.3872E+03	1.0857E+03	6.1841E+03	5.2406E+03
SCA	9.2635E+02	1.2623E+01	1.8462E+03	3.2488E+02	8.3620E+07	4.8565E+07
	F7		F8		F9	
	Avg	Std	Avg	Std	Avg	Std
MGO	**2.0255E+03**	**2.8847E+00**	**2.2242E+03**	**1.0627E+00**	2.4808E+03	1.6628E-06
MSPS	2.1189E+03	2.5761E+01	2.2407E+03	3.0445E+01	**2.4653E+03**	**1.6885E-08**
ALCP	2.0454E+03	1.7655E+01	2.2344E+03	3.0297E+01	2.4810E+03	3.4472E-01
IWO	2.1481E+03	5.1469E+01	2.2324E+03	7.9181E+00	2.4829E+03	2.6678E+00
SCAD	2.1482E+03	1.7844E+01	2.2452E+03	3.7106E+00	2.5676E+03	1.2066E+01
OBL	2.0741E+03	2.5887E+01	2.2361E+03	9.0541E+00	2.4816E+03	5.8725E-01
RIME	2.0469E+03	1.9244E+01	2.2273E+03	2.2889E+01	2.4808E+03	2.7294E-03
GWO	2.0575E+03	2.1741E+01	2.2508E+03	4.8200E+01	2.5118E+03	2.3690E+01
PSO	2.1461E+03	6.4055E+01	2.3156E+03	9.6011E+01	2.4658E+03	1.1281E-01
WOA	2.1821E+03	5.4630E+01	2.2543E+03	2.9457E+01	2.4879E+03	1.3153E+01

SCA	2.1091E+03	1.4160E+01	2.2506E+03	6.2658E+00	2.5463E+03	2.1060E+01
	F10		F11		F12	
	Avg	Std	Avg	Std	Avg	Std
MGO	**2.5023E+03**	2.9872E+01	**2.9074E+03**	2.2367E+02	**2.9391E+03**	**3.0514E+00**
MSPS	3.1345E+03	6.4983E+02	2.9167E+03	**7.4664E+01**	3.0457E+03	1.2147E+02
ALCP	2.5862E+03	1.5277E+02	2.9539E+03	3.5022E+02	2.9964E+03	3.8734E+01
IWO	3.0601E+03	4.3733E+02	2.9524E+03	1.4511E+02	2.9904E+03	3.2090E+01
SCAD	2.5410E+03	**1.0352E+01**	5.0823E+03	3.3648E+02	3.0357E+03	2.3683E+01
OBL	2.6975E+03	5.8935E+02	2.9673E+03	1.1385E+02	2.9636E+03	1.7580E+01
RIME	2.5404E+03	8.0824E+01	2.9270E+03	7.8320E+01	2.9535E+03	1.7244E+01
GWO	3.0998E+03	5.5432E+02	3.4457E+03	3.0612E+02	2.9690E+03	2.1602E+01
PSO	3.9870E+03	1.1244E+03	3.0198E+03	1.0257E+02	2.9748E+03	1.4516E+02
WOA	4.2271E+03	1.0552E+03	2.9281E+03	1.2083E+02	3.0226E+03	6.9497E+01
SCA	2.5266E+03	4.2257E+01	4.2819E+03	4.0516E+02	3.0102E+03	1.5015E+01

Table A4. Results of MGO in different dimensions.

	F1		F3		F4	
	Avg	Std	Avg	Std	Avg	Std
MG	8.0293E+	1.4444E+	**3.0006E+**	**2.1165E-**	**4.0132E+**	**1.5237E+0**
MG	2.8990E+	7.5260E+	5.2823E+	1.7689E+	4.8922E+	8.8258E+0
MG	**3.0911E+0**	**7.6396E+**	9.9102E+	1.6916E+	5.5061E+	4.0888E+0
MG	2.3298E+	6.6172E+	5.5373E+	6.5337E+	6.9006E+	4.8530E+0
	F5		F6		F7	
	Avg	Std	Avg	Std	Avg	Std
MG	**5.0395E+**	**1.4923E+**	**6.0000E+**	**8.1763E-**	**7.1457E+**	**2.1587E+0**
MG	5.5322E+	9.3729E+	**6.0000E+**	4.2859E-	7.8392E+	9.7234E+0
MG	6.3600E+	1.9806E+	**6.0000E+**	3.8432E-	8.9143E+	2.1092E+0
MG	9.9518E+	5.9381E+	6.0053E+	2.0557E-	1.4496E+	6.4696E+0
	F8		F9		F10	
	Avg	Std	Avg	Std	Avg	Std
MG	**8.0340E+**	**1.1884E+0**	**9.0000E+**	**1.9926E-**	**1.1064E+0**	**9.8556E+**
MG	8.5340E+	8.8935E+	9.0464E+	7.3657E+	3.6460E+	3.4879E+0
MG	9.3350E+	1.7090E+	1.1606E+	1.4780E+	7.4079E+	6.9213E+0
MG	1.2841E+	5.3764E+	7.0420E+	2.0584E+	1.9080E+	1.1016E+0
	F11		F12		F13	
	Avg	Std	Avg	Std	Avg	Std
MG	**1.1024E+0**	**1.7335E+**	**1.1013E+0**	**1.1564E+0**	**1.6329E+**	**8.3729E+**
MG	1.1791E+	2.2601E+	5.9778E+	4.6525E+	2.3541E+	1.8362E+0
MG	1.2698E+	3.2148E+	1.0361E+	6.1540E+	3.5202E+	5.2509E+0
MG	6.2083E+	1.4300E+	1.4222E+	5.4492E+	7.9152E+	6.7388E+0
	F14		F15		F16	
	Avg	Std	Avg	Std	Avg	Std
MG	**1.5015E+0**	**3.4950E+**	**1.6849E+**	**6.5678E+**	**1.6081E+0**	**2.4466E+**
MG	7.8529E+	4.3426E+	1.0845E+	6.4665E+	2.1474E+	1.5707E+0

MG	1.0558E+	6.5157E+	1.9092E+	1.8891E+	2.9656E+	1.5314E+0
MG	3.0724E+	1.0836E+	1.0571E+	1.0190E+	5.7371E+	3.2663E+0
	F17		F18		F19	
	Avg	Std	Avg	Std	Avg	Std
MG	**1.7045E+**	**6.8997E+**	**2.2732E+**	**5.8197E+**	**2.3327E+**	**9.8557E+**
MG	1.8590E+	4.5645E+	2.1311E+	1.0250E+	7.4845E+	6.0406E+0
MG	2.5522E+	1.4494E+	9.1593E+	5.1616E+	2.4948E+	1.8508E+0
MG	4.5936E+	2.1043E+	4.6283E+	1.7586E+	9.6082E+	1.4164E+0
	F20		F21		F22	
	Avg	Std	Avg	Std	Avg	Std
MG	**2.0028E+**	**6.1891E+0**	**2.2184E+**	3.9683E+	**2.2672E+**	**3.7070E+**
MG	2.1994E+	7.7190E+	2.3517E+	**2.0164E+**	2.7079E+	1.0437E+0
MG	2.7372E+	1.0794E+	2.4373E+	2.4612E+	8.6260E+	1.3513E+0
MG	4.5837E+	2.2528E+	2.8402E+	5.3282E+	2.1554E+	1.2922E+0
	F23		F24		F25	
	Avg	Std	Avg	Std	Avg	Std
MG	**2.6074E+**	**1.7020E+**	**2.5717E+**	7.3513E+	**2.8843E+**	4.3148E+0
MG	2.7091E+	1.5257E+	2.8748E+	4.9898E+	2.8871E+	**4.6854E-**
MG	2.8833E+	2.4126E+	3.0572E+	**2.6645E+**	3.0383E+	2.7504E+0
MG	3.2232E+	4.1746E+	3.8189E+	4.8392E+	3.3884E+	6.4698E+0
	F26		F27		F28	
	Avg	Std	Avg	Std	Avg	Std
MG	**2.8365E+**	**6.8842E+**	**3.0897E+**	**1.0022E+**	**3.0999E+**	9.0511E+0
MG	4.0186E+	3.9639E+	3.2083E+	4.4499E+	3.2194E+	**1.2742E+0**
MG	5.3556E+	2.0673E+	3.3401E+	3.3680E+	3.3295E+	9.1699E+0
MG	1.1144E+	5.3440E+	3.6093E+	4.7240E+	3.6971E+	3.6459E+0
	F29		F30			
	Avg	Std	Avg	Std		
MG	**3.1465E+**	**9.5942E+**	**5.7907E+**	**1.7869E+**		
MG	3.5823E+	9.2845E+	4.7078E+	3.9615E+		
MG	4.0899E+	1.8681E+	3.3320E+	9.0660E+		
MG	6.6377E+	2.5582E+	2.9391E+	2.0323E+		